



A high-affinity, *cis*-on photoswitchable beta blocker to optically control β_2 -adrenergic receptors *in vitro* and *in vivo*

Shuang Shi^{a,1}, Yang Zheng^{a,1}, Joëlle Goulding^{b,c}, Silvia Marri^d, Laura Lucarini^d, Benjamin Konecny^a, Silvia Sgambellone^d, Serafina Villano^d, Reggie Bosma^a, Maikel Wijtmans^a, Stephen J. Briddon^{b,c}, Barbara A. Zarzycka^a, Henry F. Vischer^a, Rob Leurs^{a,*}

^a Division of Medicinal Chemistry, Amsterdam Institute of Molecular and Life Sciences, Vrije Universiteit Amsterdam, 1081HZ Amsterdam, the Netherlands

^b Centre of Membrane Proteins and Receptors, University of Birmingham and University of Nottingham, The Midlands NG7 2UH, U.K

^c Division of Physiology, Pharmacology & Neuroscience, School of Life Sciences, University of Nottingham, Nottingham NG7 2UH, U.K

^d Department of Neurosciences, Psychology, Drug Research and Child Health (NEUROFARBA), University of Florence, Florence, 50139, Italy

ARTICLE INFO

Keywords:

β_2 AR
Photoswitchable β -blockers
GPCR signalling
Molecular modelling
Site-directed mutagenesis
Rabbit intraocular pressure

ABSTRACT

This study introduces (S)-Opto-prop-2, a second-generation photoswitchable ligand designed for precise modulation of β_2 -adrenoceptor (β_2 AR). Synthesised by incorporating an azobenzene moiety with propranolol, (S)-Opto-prop-2 exhibited a high PSS_{cis} (photostationary state for *cis* isomer) percentage (~90 %) and a favourable half-life (>10 days), facilitating diverse bioassay measurements. *In vitro*, the *cis*-isomer displayed substantially higher β_2 AR binding affinity than the *trans*-isomer (1000-fold), making (S)-Opto-prop-2 one of the best photoswitchable GPCR (G protein-coupled receptor) ligands reported so far. Molecular docking of (S)-Opto-prop-2 in the X-ray structure of propranolol-bound β_2 AR followed by site-directed mutagenesis studies, identified D113^{3,32}, N312^{7,39} and F289^{6,51} as crucial residues that contribute to ligand-receptor interactions at the molecular level. *In vivo* efficacy was assessed using a rabbit ocular hypertension model, revealing that the *cis* isomer mimicked propranolol's effects in reducing intraocular pressure, while the *trans* isomer was inactive. Dynamic optical modulation of β_2 AR by (S)-Opto-prop-2 was demonstrated in two different cAMP bioassays and using live-cell confocal imaging, indicating reversible and dynamic control of β_2 AR activity using the new photopharmacology tool.

In conclusion, (S)-Opto-prop-2 emerges as a promising photoswitchable ligand for precise and reversible β_2 AR modulation with light. The new tool shows superior *cis*-on binding affinity, one of the largest reported differences in affinity (1000-fold) between its two configurations, *in vivo* efficacy, and dynamic modulation. This study contributes valuable insights into the evolving field of photopharmacology, offering a potential avenue for targeted therapy in β_2 AR-associated pathologies.

Abbreviations: β ARs, β -adrenergic receptors; BPMC, Biased Probability Monte Carlo; BSA, Bovine Serum Albumin; DEA, diethanolamine; DHA, Dihydroalprenolol; DMSO, dimethyl sulfoxide; DMEM, Dulbecco's Modified Eagle Medium; DMF, dimethylformamide; EPAC, exchange protein activated by 3'-5'-cyclic adenosine monophosphate [cAMP]; EDTA, Ethylenediaminetetraacetic acid; ESI, electrospray ionization; FI, fluorescent; FBS, Fetal Bovine Serum; FDA, Food and Drug Administration; FRET, fluorescence resonance energy transfer; GPCR, G protein-coupled receptor; HCl, hydrogen chloride; HBSS, Hank's Balanced Salt Solution; HRMS, high resolution mass spectrometry; HSQC, heteronuclear single quantum correlation; HMBC, heteronuclear multiple bond correlation; HPLC, High-Performance Liquid Chromatography; IOP, Intraocular pressure; LC-MS, Liquid chromatography–mass spectrometry; NMR, Nuclear Magnetic Resonance; OHT, Transient ocular hypertension; PBS, Dulbecco's phosphate-buffered saline; PSS, photostationary state; PEI, polyethyleneimine; ppm, parts per million; TLC, Thin Layer Chromatography; TEA, triethanolamine; RT, room temperature; UV-Vis, Ultraviolet-visible; sSNAP-AF488, SNAP-Surface Alexafluor 488.

* Corresponding author.

E-mail address: r.leurs@vu.nl (R. Leurs).

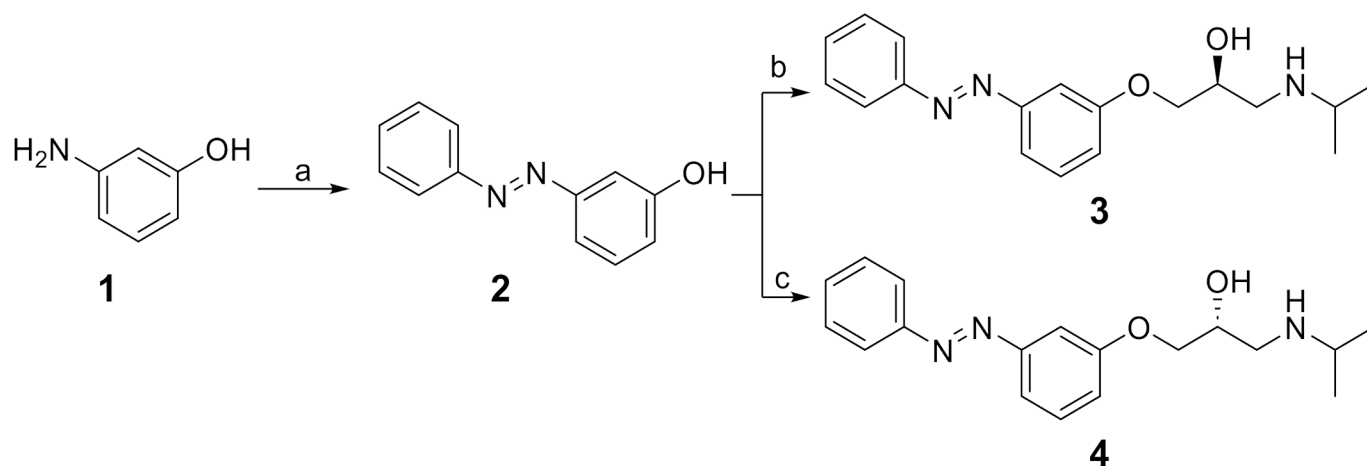
¹ Both authors contributed equally.

<https://doi.org/10.1016/j.bcp.2024.116396>

Received 23 April 2024; Received in revised form 7 June 2024; Accepted 25 June 2024

Available online 26 June 2024

0006-2952/© 2024 The Authors. Published by Elsevier Inc. This is an open access article under the CC BY license (<http://creativecommons.org/licenses/by/4.0/>).



Scheme 1. Synthetic routes of the photoswitchable (*S*)-Opto-prop-2 (3, VUF25474) and (*R*)-Opto-prop-2 enantiomers (4, VUF25475). Reagents and conditions: a) PhNO, AcOH, RT (room temperature), overnight, 14 %; (b) i) NaH, (*S*)-epichlorohydrin, DMF, 0 °C to RT, overnight; ii) ¹PrNH₂, RT, 1 h, 38 %; (c) i) NaH, (*R*)-epichlorohydrin, DMF, 0 °C to RT, overnight; ii) ¹PrNH₂, RT, 1 h, 23 %.

1. Introduction

Photopharmacology is an emerging and promising strategy in which the bioactivity of photosensitive ligands on their biological target is controlled by light. The ability to activate and/or deactivate photosensitive ligands with light of specific wavelengths provides precise control of the location (spatial) and duration (temporal) of their bioactivity, which might attenuate on-target adverse effects *in vivo* by only regulating the target in diseased tissues without affecting the target elsewhere in the body [1–3]. Photosensitive ligands can be subdivided into two main groups: 1) photocaged ligands, in which a ligand is inactivated (caged) by a photoreactive moiety from which it can be irreversibly released by light (uncaging), resulting in the active parent ligand [4] and 2) photoswitchable ligands, in which a ligand can reversibly change its shape due to the introduction of a light-sensitive moiety that can isomerize between different configurational states upon illumination [4,5].

Approximately 35 % of FDA (Food and Drug Administration) approved drugs target GPCRs [6]. As one of the best-characterised members of the GPCR family, β -adrenergic receptors (β ARs) have also appeared as major targets for drug development. There are three subtypes of β ARs, β_1 AR, β_2 AR and β_3 AR. β_1 AR and β_2 AR are ubiquitously expressed in many tissues and are crucial molecular targets in multiple diseases, including asthma, cardiac disorders, and hypertension, whereas β_3 AR is mainly expressed in adipose tissues and regulates metabolic processes [8]. Various β AR-antagonists (so-called β -blockers) have been successfully applied in the clinical treatment of heart failure, ischemic heart disease, arrhythmia for decades and are also part of the therapeutic arsenal for infantile hemangiomas, retinopathy of prematurity, and glaucoma [7–9]. In view of such tissue-dependent functions, the localized modulation of β ARs is potentially a promising innovative strategy for new therapeutic interventions.

Recently, the first photosensitive β -blocker analogues have been reported. For example, caging carvedilol with a coumarin moiety impaired its antagonistic effect on β -adrenoceptor *in vitro*, *ex vivo* and *in vivo*, which was readily restored upon uncaging with visible light [10]. In addition, azologization of (*S*)-propranolol by substituting its naphthalene with a *para*-acetamido azobenzene yielded the photoswitchable β_2 AR antagonist Photoazolol-1 with a 17-fold higher inhibitory potency for the *trans* isomer as compared to the PSS_{cis} [11]. In contrast to Photoazolol-1, in which the propranolol side chain is on the *ortho*-position of azobenzene, the *meta*- and *para*-substituted analogues Photoazolol-2 and -3 displayed only a 3.7-fold difference in inhibitory potency between *trans* and PSS_{cis} states, or no inhibitory potency,

respectively. Interestingly, replacing the naphthalene of propranolol with an unsubstituted azobenzene moiety at the *meta* position yielded the *cis*-active photoswitchable β_2 AR antagonist Opto-prop-2 (VUF17062) with an almost 600-fold increased binding affinity upon illumination at 360 nm [12], whereas the *ortho*- and *para*-substituted analogues showed < 5-fold affinity shift upon photoswitching. As Opto-prop-2 is a racemic mixture, we hypothesized that its *S*- or *R*-enantiomer might display further improved photopharmacological properties. In this study, the two enantiomers of Opto-prop-2 were synthesised and characterized with respect to photochemistry and *in vitro* and *in vivo* (photo)pharmacology. In addition, molecular docking studies and site-directed mutagenesis were performed to rationalize the large affinity switch between the *trans* and *cis* isomers.

2. Material and Methods

2.1. Materials

Dulbecco's Modified Eagle Medium (DMEM, #41966–029), Trypsin (#25300–054), Penicillin Streptomycin (Pen Strep, #15140–122) and Hank's Balanced Salt Solution (HBSS, #14025–050) were obtained from Thermo Fisher Scientific (Paisley, United Kingdom). Fetal Bovine Serum (FBS, # S00E110004) was from BODINCO BV (Alkmaar, the Netherlands). Hygromycin B (#10687010) and Zeocin (#ant-an-1) were purchased from Invivogen (Toulouse, France). Dulbecco's phosphate-buffered saline (PBS, #D8662-6X500 mL), Poly-L-lysine (#P8920-500 mL), poly-D-lysine (#P6407-5 mg) and Poly(ethyleneimine) solution (branched PEI, #P3141) were obtained from Sigma-Aldrich (Missouri, United States). Linear polyethyleneimine (PEI, #23966–5) was obtained from Polysciences (Warrington, United States). White 96-well plate (#655083) and black-transparent 96-well plate (#655090) were obtained from Greiner (Alphen aan den Rijn, the Netherlands). DMEM complete medium was made up of DMEM supplemented with 10 % FBS and 1 % Pen Strep. Furimazine (NanoGlo®, #N1130) was from Promega Benelux (Leiden, the Netherlands). [³H] Dihydroalprenolol ([³H] DHA, #NET720250UC) and MicroScint™-O (#6013611) were obtained from Revvity (Groningen, the Netherlands). TRIS Base (#T60040-5000.0) was purchased from MELFORD (Ipswich, United Kingdom). Propranolol and racemic Opto-prop-2 (VUF17062) were synthesized in-house as previously reported [12]. All the other compounds were purchased from Sigma-Aldrich (Amsterdam, the Netherlands) or Thermo Fisher Scientific (Breda, the Netherlands).

2.2. Photochemistry

UV-Vis (Ultraviolet-visible) spectra were monitored using a Thermo-scientific Evolution 201 PC spectrophotometer. Illumination was executed using a Sutter Instruments Lambda LS with a 300 W full-spectrum lamp connected to a Sutter Instruments Lambda 10–3 optical filter changer equipped with 434 ± 9 nm and 360 ± 20 nm filters with a light intensity of 0.79 mW/mm² and 0.93 mW/mm² respectively. Intensities were obtained using a Thorlabs PM100D power energy meter. Multiple isomerization cycles were measured by measuring absorbance at 320 nm with an intensity of 5 % using the Sutter Instrument Lambda 721.

PSS_{cis} and PSS_{trans} values were determined by UV spectroscopy in Hellma Suprasil quartz 114-QS cuvettes. A solution of each compound in 1 % DMSO (dimethyl sulfoxide)/HBSS (Hank's Balanced Salt Solution) (25 μM) in a vial was illuminated to PSS_{cis} with 360 nm for 10 min and subsequently to PSS_{trans} with 434 nm for 10 min. Thermal relaxation experiments were performed according to Priimagi et al [13] using a compound concentration of 25 μM in HBSS buffer/1% DMSO and temperatures of 60, 70, and 80 °C. Following Arrhenius extrapolations, the relaxation half-life at room temperature was calculated.

Illuminations of compounds for the pharmacological experiments of this study were performed at room temperature in cylindrical clear glass vials with a volume of 4 mL for 10 min with a 360 nm or 434 nm filter. Samples were 10 mM in DMSO. The photoisomerization and photostability were monitored by LCMS (liquid chromatography–mass spectrometry) for all the samples. The typical distance between the light source and the vials or cuvettes was 2 cm. All the experiments were performed under red light.

2.2.1. Synthesis and characterization of compounds

All starting materials were obtained from commercial suppliers and used without purification. For the synthesis of the two enantiopure isomers a similar synthetic route (Scheme 1) was followed. The preparation of Opto-prop-2 and **2** was reported previously [12]. Anhydrous DMF (dimethylformamide) was obtained by passing through an activated alumina column before use. All reactions were carried out under a nitrogen atmosphere unless mentioned otherwise. TLC (Thin Layer Chromatography) analyses were performed using Merck F₂₅₄ aluminium-backed silica plates and visualized with 254 nm UV light. Flash column chromatography was executed using Biotage Isolera equipment. All HRMS (high resolution mass spectrometry) spectra were recorded on a Bruker microTOF mass spectrometer using ESI (electrospray ionization) in positive-ion mode. Optical rotation was measured with the P3000 polarimeter from Krüss Optronic GmbH. NMR (Nuclear magnetic resonance) spectra were determined with a Bruker Avance II 500 MHz or a Bruker Avance III HD 600 MHz spectrometer. Chemical shifts are reported in parts per million (ppm) against the reference compound using the signal of the residual non-deuterated solvent (CDCl₃ δ = 7.26 ppm (¹H), δ = 77.16 ppm (¹³C); DMSO-*d*₆ δ = 2.50 ppm (¹H), δ = 39.52 ppm (¹³C)). NMR spectra were processed using MestReNova 14.0 software. The peak multiplicities are defined as follows: s, singlet; d, doublet; t, triplet; q, quartet; dd, doublet of doublets; ddd, doublet of doublets of doublets; dt, doublet of triplets; dq, doublet of quartets; td, triplet of doublets; tt, triplet of triplets; qd, quartet of doublets; p, pentet; dp, doublet of pentets; br, broad signal; m, multiplet.

For NMR listings, the following additional procedures were used: 1) Multiplicity is not solely reported based on peak shapes, but also distinguishes the coupling to all non-equivalent protons that have similar *J* values; 2) If additional smaller couplings are observed but are too small for accurate quantitation because the precision is smaller than the digital resolution, a symbol ^Δ will be used; 3) The notation 'm' is used in case of obscured accurate interpretation as a result of (i) overlapping signals for different protons, or (ii) a result of overlapping signal lines within the same proton signal; 4) For any rotamers or diastereomers, signals will be listed separately; 5) NMR signals that could only be

detected with HSQC (heteronuclear single quantum correlation) analysis are denoted with a # symbol; 6) NMR signals that could only be detected with HMBC (heteronuclear multiple bond correlation) analysis are denoted with a * symbol; 7) Signals for exchangeable proton atoms (such as NH and OH groups) are only listed if clearly visible (excluding e. g. the use of D₂O or CD₃OD) and if confirmed by a D₂O shake and/or HSQC. It should be noted that not all ¹³C signals are visible in the spectra due to the tautomerism of non-N-substituted pyrazoles. HSQC and HMBC were measured to assign ¹³C signals if applicable. Purities were measured using analytical LC-MS (liquid chromatography–mass spectrometry) using a Shimadzu LC-20AD liquid chromatography pump system with a Shimadzu SPDM20A diode array detector with the MS detection performed with a Shimadzu LCMS-2010EV mass spectrometer operating in positive ionization mode. The column used was an Xbridge (C18) 5 μm column (100 mm × 4.6 mm). The following solutions are used for the LC-MS eluents. Solvent A: H₂O/HCOOH 999:1, and solvent B: MeCN/HCOOH 999:1. The eluent program used is as follows: flow rate: 1.0 mL/min, start with 95 % A in a linear gradient to 10 % A over 4.5 min, hold 1.5 min at 10 % A, in 0.5 min in a linear gradient to 95 % A, hold 1.5 min at 95 % A, total run time: 8.0 min. Compound purities were calculated as the percentage peak area of the analyzed compound by UV detection at 254 nm. All final compounds are > 95 % pure by HPLC (High-Performance Liquid Chromatography) analysis. For the separation of Opto-prop-2 enantiomers, an isocratic eluent of 10 % ⁱPrOH in heptane with 0.1 % DEA (diethanolamine) running at 1 mL/min for 30 min on Cellulose 3 (250 × 4.6 mm) chiral column at room temperature was used.

(*S,E*)-1-(Isopropylamino)-3-(3-(phenyldiazenyl)phenoxy)propan-2-ol (**3**, (*S*)-Opto-prop-2, VUF25474).

To a slurry of NaH (44 mg, 1.1 mmol, 1.1 eq) in DMF (3.0 mL) at 0 °C was added dropwise a solution of **2** (0.20 g, 1.0 mmol, 1.0 eq) in DMF (0.5 mL). When the H₂ evolution stopped, (S)-epichlorohydrin (0.23 g, 1.0 mmol, 1.0 eq) in DMF (0.5 mL) was added dropwise at 0 °C. After 16 h at RT (room temperature), ⁱPrNH₂ (0.87 mL, 0.10 mol, 10 eq) was added and the mixture was stirred at RT for 1 h. The reaction mixture was concentrated *in vacuo* and the mixture was partitioned between aq. satd. Na₂CO₃ (5 mL) and EtOAc (5 mL). The organic phase was washed with brine (5 mL), dried over anhydrous Na₂SO₄, filtered and evaporated *in vacuo*. The compound was purified by flash column chromatography on silica gel with a gradient elution of EtOAc in cyclohexane (50 % – 100 %) with 2 % TEA (triethanolamine) to get the title compound as an orange solid (73 mg, 23 %). ¹H NMR (500 MHz, DMSO-*d*₆) δ 7.93–7.87 (m, 2H), 7.64–7.55 (m, 3H), 7.54–7.48 (m, 2H), 7.44–7.40 (m, 1H), 7.19–7.13 (m, 1H), 5.01 (s, 1H), 4.08 (dd, *J* = 9.7, 4.4 Hz, 1H), 3.97 (dd, *J* = 9.7, 6.2 Hz, 1H), 3.91–3.84 (m, 1H), 2.75–2.66 (m, 2H), 2.58 (dd, *J* = 11.7, 6.7 Hz, 1H), 1.58 (br s, 1H), 0.99 (d, *J* = 1.6 Hz, 3H), 0.97 (d, *J* = 1.6 Hz, 3H); ¹³C NMR (151 MHz, DMSO-*d*₆) δ 159.6, 153.1, 151.8, 131.6, 130.3, 129.5, 122.6, 118.3, 116.4, 106.5, 71.1, 68.4, 49.9, 48.2, 22.99, 22.96; LC-MS: t_R = 3.56 min, purity: >99 %, *m/z* [M + H]⁺ 314; HRMS: calc. for C₁₈H₂₃N₃O₂ [M + H]⁺: 314.1863, found: 314.1871. Chiral HPLC: t_R = 14.9 min, ee 92 %, [α]_D²² = -20.0 (c = 1.0, MeOH).

(*R,E*)-1-(Isopropylamino)-3-(3-(phenyldiazenyl)phenoxy)propan-2-ol (**4**, (*R*)-Opto-prop-2, VUF25475).

This compound was produced following the same protocol as for **3** but using (R)-epichlorohydrin to yield the title compound as an orange solid (120 mg, 38 %). ¹H NMR (600 MHz, DMSO-*d*₆) δ 7.92–7.88 (m, 2H), 7.63–7.56 (m, 3H), 7.53–7.49 (m, 2H), 7.43–7.40 (m, 1H), 7.18–7.14 (m, 1H), 5.01 (s, 1H), 4.08 (dd, *J* = 9.7, 4.4 Hz, 1H), 3.97 (dd, *J* = 9.7, 6.2 Hz, 1H), 3.91–3.84 (m, 1H), 2.75–2.66 (m, 2H), 2.58 (dd, *J* = 11.7, 6.8 Hz, 1H), 0.99 (d, *J* = 2.0 Hz, 3H), 0.98 (d, *J* = 2.0 Hz, 3H); ¹³C NMR (151 MHz, DMSO-*d*₆) δ 159.6, 153.1, 151.8, 131.6, 130.3, 129.5, 122.6, 118.3, 116.4, 106.5, 71.1, 68.4, 49.9, 48.2, 23.0, 22.9; LC-MS: t_R = 3.46 min, purity: 97.7 %, *m/z* [M + H]⁺ 314; HRMS: calc. for C₁₈H₂₃N₃O₂ [M + H]⁺: 314.1863, found: 314.1874. Chiral HPLC: t_R =

11.9 min, ee 93 %. $[\alpha]_D^{22} = +16.0$ ($c = 1.0$, MeOH).

2.3. Pharmacology

2.3.1. Constructs

Human β_1 AR and β_2 AR (GenBank: NP_000675.1 and NP_000015.1, respectively) in pcDEF3 and pcDNA3.1 + expression plasmids have been previously described [12]. All β_2 AR mutants were generated by polymerase chain reaction (PCR)-mediated mutagenesis and subcloned into pcDNA3.1 + expression plasmid. LgBiT- β arrestin2 was a kind gift from Dr. J.Y. Seong (Korea University, Seoul, Republic of Korea) [14]. The cDNA coding for the human β_2 AR fused in frame to SmBiT synthesized by Biomatik (Delaware, the United States) via a linker (TSSGSSGGGGSGGGGSSG) [15] and was subcloned in pcDEF3 expression plasmid. All generated constructs were verified by DNA sequencing.

2.3.2. Radioligand binding studies

2.3.2.1. Membrane production. Two million HEK293T cells (ATCC, CRL-1573) were seeded in a 10 cm² tissue-culture dish in DMEM supplemented with 10 % FBS and penicillin (100 IU/mL) and cultured in a humidified incubator at 37 °C with 5 % CO₂. The next day, cells were transiently transfected with 1 μ g β_1 AR or β_2 AR plasmids and 4 μ g empty pcDEF3 plasmid using 30 μ g 25 kDa linear polyethyleneimine. After 48 h, cell membranes were prepared as previously described [12]. Briefly, cells were washed twice with ice-cold PBS and centrifuged at 1500 g. The cell pellets were resuspended in ice-cold Tris-HCl (hydrogen chloride) buffer (15 mM, supplemented with 0.3 mM EDTA (Ethylenediaminetetraacetic acid) and 2 mM MgCl₂ at pH 7.4) and subsequently homogenized by plunging a pestle 10 times (Tamson, the Netherlands). The homogenates were twice frozen-thawed using liquid-nitrogen and membranes were collected with ultra-centrifugation at 40,000 g. The protein content was determined by using a BCA protein assay kit (Thermo Scientific, the United States).

2.3.2.2. Radioligand binding assay. The saturation binding assay was conducted on 0.8–15 μ g membranes expressing mutant β_2 AR with 0–25 nM [³H] DHA in 100 μ L binding buffer (HBSS containing 0.1 % BSA (Bovine Serum Albumin)) for 1 h at 25 °C. Non-specific binding was measured in the presence of 100 μ M propranolol. Radioligand displacement experiment was carried out on 0.1–15 μ g membranes expressing β_1 AR, β_2 AR or mutant β_2 AR using 0.8–4 nM [³H] DHA in combination increasing concentrations of propranolol or pre-illuminated photoswitchable ligands (pre-illuminated with 360 or 434 nm for 10 mins) in 100 μ L binding buffer (HBSS containing 0.1 % BSA) for 1 h at 25 °C. Incubations were terminated by rapid filtration over a 0.5 % PEI (branched PEI)-coated 96-well GF/C filter plate followed by three rapid wash steps with ice-cold wash buffer (50 mM Tris-HCl and 500 mM NaCl, pH 7.4) using a Perkin Elmer 96-well harvester (Perkin Elmer, Groningen, the Netherlands). The GF-C filter plates were dried at 52 °C for 1 h and 25 μ L Microscint-O scintillation liquid was added per well. Filter-bound radioactivity was measured using a Microbeta Wallac Trilux scintillation counter (Perkin Elmer, Groningen, the Netherlands) after a 120-minute delay.

2.3.3. Confocal imaging

HEK293T cells expressing an N-terminal SNAP-tagged β_2 AR, created as described [16] using a pSIN-B2-BSD(GE) lentiviral construct, were seeded at a density of 30,000 cells/well in a clear-bottom black Greiner 96-well plate (#655096) in DMEM complete medium and left overnight in a humidified incubator at 37 °C with 5 % CO₂. The following day media was replaced with 0.5 μ M SNAP-Surface Alexafluor 488 (sSNAP-AF488; NEB) in the growth medium and incubated for 30 min at 37 °C before being exchanged for HEPES-buffered saline solution (145 mM NaCl, 5 mM KCl, 1.3 mM CaCl₂, 1 mM MgSO₄, 10 mM HEPES, 2 mM

sodium pyruvate, 1.5 mM NaHCO₃, and 10 mM D-glucose, pH 7.45). Cells were pre-incubated for 30 min at 37 °C in the presence of 1 μ M PSS_{cis} (S)-Opto-prop-2, 1 μ M *trans* (S)-Opto-prop-2 or HEPES-buffered saline solution alone prior to UV illumination utilising the Cell Discoverer 7 (Zeiss). Each UV-illuminated well was exposed to 3 min of 385 nm LED at full power (6 separate 3.6 × 2.9 mm tiled fields of view for an exposure time of 30 s each) using a 5x Plan-Aprochromat 0.35NA air objective and a 1x tube lens. 10 nM of a fluorescent ICI₁₁₈₋₅₅₁ analogue [17] was then added to all wells and incubated for 30 min at 37 °C before confocal images were captured on the Cell Discoverer 7. sSNAPAF488 and fluorescent ICI₁₁₈₋₅₅₁ were imaged utilising 488 nm and 640 nm excitation, with 410–617 nm and 646–700 nm emission bandwidths respectively with a 20x Plan-Apochromat 0.95NA air objective and 1x tube lens. Experiments were carried out in triplicate with the mean membrane intensity of bound fluorescent ICI₁₁₈₋₅₅₁ determined from 3 separate fields of view per well. Imaging laser powers gain and offset settings were kept consistent between experiments.

2.3.4. Molecular docking

The (S)-Opto-prop-2 *cis* and *trans* isomers were docked into the propranolol-bound human β_2 -adrenergic receptor X-ray structure (PDB ID: 6PS5) [18] using an energy-based docking protocol implemented in the ICM-Pro software [19]. Compounds were generated from 2D representations, and their 3D geometry was optimized using a MMFF-94 force field. The docking was performed in the rectangular box that comprised the orthosteric binding pocket. Docking simulations used BPMC (Biased Probability Monte Carlo) optimization of the compounds' internal coordinates in the pre-calculated grid energy potentials of the receptor. The exhaustive sampling of the compound conformational space was done with the thoroughness parameter set to 10 and performing at least three independent docking runs for each compound. The final docking poses were selected based on optimal interactions between propranolol and β_2 AR and ICM binding scores. The figures were generated using PyMOL Molecular Graphics System, Version 2.5.4 Schrödinger, LLC (<https://pymol.org>).

2.3.5. NanoBiT luminescence β arrestin2 recruitment assay

One million HEK293T cells were transiently transfected in suspension with 400 ng β_2 AR-SmBiT, 600 ng LgBiT- β arrestin2 and 1000 ng empty plasmids using 12 μ g linear PEI in DMEM complete medium, and subsequently seeded (30,000 cells/well) in white 96-well plates. After 48 h, cells were washed and pre-incubated with HBSS buffer and antagonists (Opto-prop-2 isomers or propranolol) for 10 min at 37 °C, followed by the addition of furimazine (312-fold dilution from stock) and isoprenaline. The total luminescence was measured in a PHERAstar plate reader (BMG Labtech) after 30 mins incubation at 37 °C.

2.3.6. In vivo transient ocular hypertension model

The experimental procedures were carried out in New Zealand albino rabbits. All procedures on animals conformed to the Association for Research in Vision and Ophthalmology Resolution, in agreement with the Good Laboratory Practice for the use of animals, with the European Union Regulations (Directive 2010/63/EU), upon authorization of the National Ethics Committee of the Italian Ministry of Health (number 110/2021-PR). Male albino rabbits (body weight 2–2.5 kg) were kept in individual cages; food and water were provided ad libitum. The animals were maintained on a 12–12 h light/dark cycle in a temperature-controlled room (22–23 °C). Animals were identified with a tattoo on the ear, numbered consecutively. All selected animals underwent ophthalmic and general examinations before the beginning of the study. A total of 12 rabbits were used for the parallel study of each of the four compounds and for the vehicle.

The ocular surface of New Zealand white rabbits was locally anaesthetised by one drop of 0.4 % oxybuprocaine hydrochloride [20]. Transient ocular hypertension (OHT) was induced by bilateral injection of 50 μ L sterile hypertonic saline (5 %) into the vitreous as previously

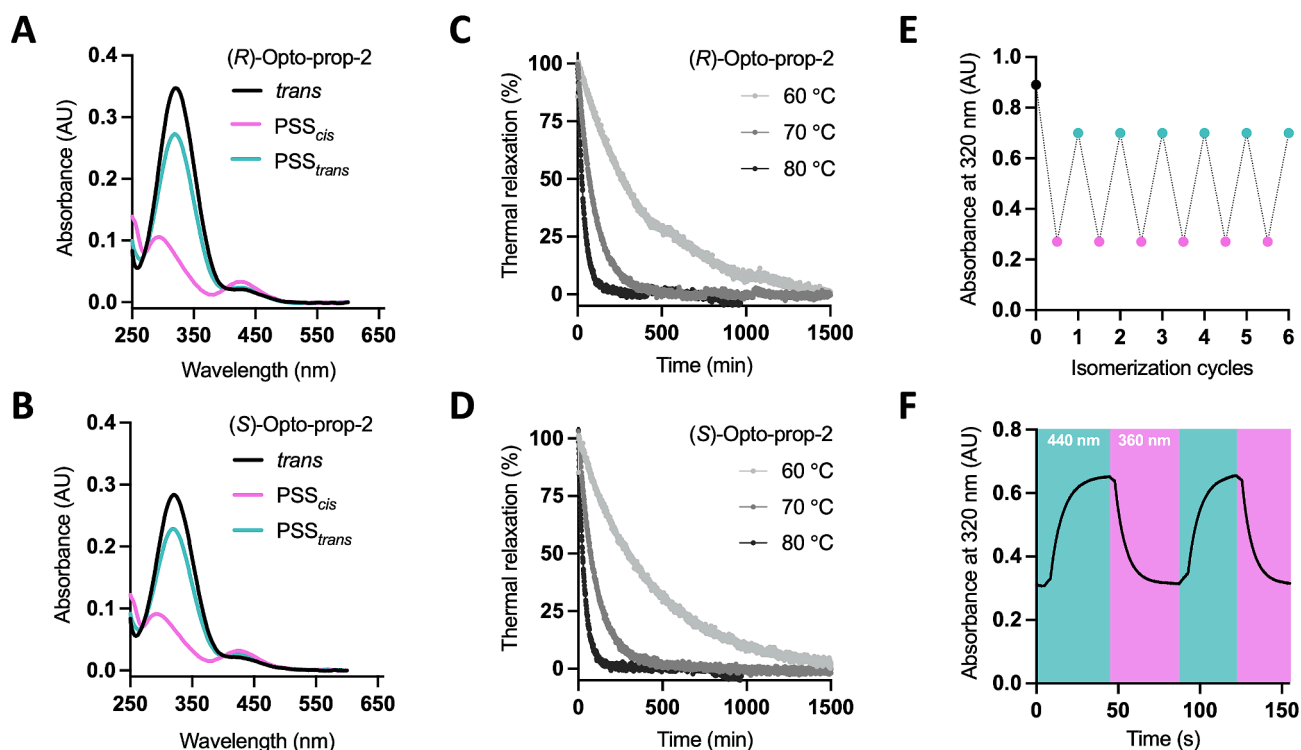


Fig. 1. Photochemical characterization of photoswitchable (R)-Opto-prop-2 and (S)-Opto-prop-2 enantiomers. UV-Vis spectroscopy analysis in 1 % DMSO/HBSS buffer of 25 μ M (R)-Opto-prop-2 (A) and (S)-Opto-prop-2 (B) *trans* (black lines), PSS_{cis} upon illumination with 360 nm for 10 mins (magenta line), and PSS_{trans} upon subsequent illumination of *cis* isomer with 434 nm (cyan line). (C, D) Thermal relaxation of (R)-Opto-prop-2 (C) and (S)-Opto-prop-2 (D) *cis* isomers to the more stable *trans* isomers. (E) Dynamic switching of 25 μ M (S)-Opto-prop-2 in 1 % DMSO/HBSS buffer was measured by UV-Vis spectroscopy at 1-second intervals under alternating illumination (2 min for each illumination) with 360 nm and 440 nm perpendicular to the light source of the UV-Vis spectrometer. (F) Repeated isomerization cycles between PSS_{cis} (magenta) and PSS_{trans} (cyan) of 25 μ M (S)-Opto-prop-2 in 1 % DMSO/HBSS buffer measured at 320 nm upon alternating illumination with 360 and 440 nm.

described [20]. Drops of 0.05 % vehicle and ligands in phosphate buffer with 10 % cremophor were instilled in the ocular cul-de-sac 10 min post saline addition. Intraocular pressure (IOP) was measured using a Model 30™ Pneumatometer (Reichert Inc. Depew, NY). One drop of 0.4 % oxybuprocaine hydrochloride was instilled in each eye immediately before each set of pressure measurements. The change in IOP was determined as the discrepancy between the average value of IOP with different treatments and the average value of IOP in vehicles at relative time points.

2.3.7. Dynamic modulation of isoprenaline-induced β_2 AR signaling by (S)-Opto-prop-2 using light

2.3.7.1. FRET-based EPAC cAMP assay. HEK293 cells stably expressing a cAMP FRET (fluorescence resonance energy transfer) biosensor consisting of EPAC (exchange protein activated by 3'-5'-cyclic adenosine monophosphate [cAMP]) fused to the FRET pair mCerulean and mCitrine have been previously described and were kindly provided by Dr. M Zimmermann (InterAx Biotech, Switzerland) [21]. The cell line was maintained in DMEM complete medium supplemented with 0.06 mg/mL Zeocin in a humidified incubator at 37 °C with 5 % CO₂. The day before the assay, cells were seeded (100,000 cells/well) in a black-transparent 96-well plate. Next, the culture medium was replaced with HBSS containing either 10 nM (S)-Opto-prop-2 *trans* or propranolol in combination with 24 nM isoprenaline and incubated in the dark for 45 min at 25 °C (increasing concentrations of compounds were applied to obtain the dose-response curves). FRET was measured in the CLARIOstar Plus plate reader (BMG Labtech, Germany) using 430–15 nm excitation, 480–20 and 530–20 nm emission wavelengths. Next, the cells were continuously illuminated with the 365 nm (0.51 mW/cm²) LED

array plate (LEDA-365, Teleopto, Japan) in constant mode for 10 min followed by FRET measurement. The cells were then illuminated with the 430 nm (1.4 mW/cm²) LED array plate (LEDA-430, Teleopto, Japan) in constant mode for 10 min followed by FRET detection. This alternating illumination and FRET detection procedure was repeated two more rounds to evaluate the reversibility of (S)-Opto-prop-2 switching over time. FRET ratio was calculated as acceptor (530 nm) divided by donor (480 nm) signals and subsequently normalized to the vehicle (0 %) and isoprenaline (100 %) responses.

2.3.7.2. Red-upward cADDIS™ cAMP sensor assay. HEK293T cells (50,000 cells/well) were transfected with 2×10^5 viral genes of Red-upward cADDIS™ sensor BacMam (#U0200, Montana Molecular, the United States) and 10^4 viral genes of β_2 AR BacMam (#Z0500N, Montana Molecular, the United States) 150 μ L DMEM complete medium supplemented with 300 nM sodium butyrate. Cells were seeded in poly-D-lysine-coated black-transparent plates and cultured in a humidified incubator at 37 °C with 5 % CO₂ [22]. After 20–24 h, culture medium was replaced with PBS and baseline fluorescent intensity (FI) was measured in the CLARIOstar plate reader (BMG Labtech, Germany) using 566 nm excitation and 620 nm emission wavelengths. Cells were then incubated with 0.3 nM isoprenaline in combination with either 100 nM (S)-Opto-prop-2 *trans* or propranolol for 45 min at 25 °C. Next, FI was measured, followed by three cycles of alternating illumination with 365 and 430 nm LED array plates as described above and FI detections. FI values were divided by baseline FI for each well, and data were then normalized to observed effects of 0.3 nM isoprenaline (100 %) and the vehicle (0 %).

Table 1
Photochemical characterization of photoswitchable Opto-prop-2 *S*- and *R*-enantiomers.

compounds	λ_{\max} <i>trans</i> ^[a] (nm)	λ_{\max} <i>cis</i> ^[a] (nm)	Isosbestic point ^[a] (nm)	PSS _{<i>cis</i>} ^[b] (cis area%)	PSS _{<i>trans</i>} ^[b] (cis area%)	t _{1/2} at 20 °C ^[c]
(<i>S</i>)-Opto-prop-2 (VUF25474)	322	425	269/401	89.4 ± 0.6	19.5 ± 0.1	>10 day
(<i>R</i>)-Opto-prop-2 (VUF25475)	322	425	270/402	89.1 ± 0.4	18.9 ± 0.1	>10 day

^[a] extracted from UV–Vis spectra (25 μM in HBSS buffer with 1 % DMSO). ^[b] measured in DMSO (10 mM) after illumination with 360 nm to PSS_{*cis*} at room temperature and defined as the percentage of the area of the *cis* isomer detected by LCMS analysis at the corresponding isosbestic point wavelength. ^[c] as approximated from the thermal relaxation of a PSS_{*cis*} sample (25 μM in HBSS buffer with 1 % DMSO) with the Arrhenius method and extrapolation to the indicated temperature.

Table 2
Receptor binding affinities of photoswitchable Opto-prop-2 *S*- and *R*-enantiomers.

compound	β_1 AR pK _i ^[a] <i>trans</i>	pK _i ^[a] PSS _{<i>cis</i>} ^[b]	Δ pK _i ^[c]	β_2 AR pK _i ^[a] <i>trans</i>	pK _i ^[a] PSS _{<i>cis</i>}	Δ pK _i
propranolol	9.4 ± 0.2 (7)	N/A	N/A	9.8 ± 0.1 (8)	N/A	N/A
racemic Opto-prop-2 (VUF17062) ^[d]	5.3 ± 0.1 (3)	6.7 ± 0.0 (3)	1.3 ± 0.0	5.8 ± 0.3 (3)	8.6 ± 0.3 (3)	± 0.5
(<i>S</i>)-Opto-prop-2 (VUF25474)	5.5 ± 0.1 (3) ns, p=0.1739	6.9 ± 0.0 (3) *, p=0.0281	1.4 ± 0.1	5.5 ± 0.1 (4) ns, p=0.0819	8.5 ± 0.2 (4) ns, p=0.9618	± 0.2
(<i>R</i>)-Opto-prop-2 (VUF25475)	5.2 ± 0.1 (3) ns, p=0.3563	5.4 ± 0.1 (3) ****, p<0.0001	0.2 ± 0.1	5.1 ± 0.1 (4) ****, p=0.0005	7.1 ± 0.4 (4) ****, p=0.0005	± 0.5

^[a] data are shown as mean ± SD of ≥ 3 experiments (indicated between parentheses) performed in triplicate. ^[b] compounds were pre-illuminated with 360 nm to PSS_{*cis*} before experimentation. ^[c] difference in pK_i between *trans* and PSS_{*cis*}. N/A = not applicable. ^[d] data were from [12]. Statistic differences between racemic Opto-prop-2 and the two enantiomers were analyzed using One-way ANOVA with Dunnett's multiple comparisons test, ns = not significant.

2.3.8. Data analysis

Data were analysed by nonlinear regression analysis using GraphPad Prism 10.0.1 and image analysis was performed in Zen Black (2012 SP5). EC₅₀ or IC₅₀ values were obtained by fitting the data to a nonlinear regression with the application of Global fitting. The K_i or K_b values of ligands were determined using the Cheng-Prusoff equation using the concentration of radioligand or agonist in combination with K_d or EC₅₀ values, respectively. Data were normalized to the effect of the vehicle (0 %) and the maximum response obtained with isoprenaline (100 %). Each figure represented the pooled data from at least three independent experiments performed in triplicate.

3. Results

3.1. Synthesis and photochemical properties of Opto-prop-2 *S*- and *R*-enantiomers

Previously we showed that the racemic Opto-prop-2 was a high-affinity, *cis*-on photoswitchable β_2 AR antagonist [12]. In this study, we synthesized both the *S*- and *R*-enantiomer of the photoswitchable propranolol analogue using similar routes as used for Opto-prop 2 (Scheme 1 in Materials and Methods). Both (*R*)-Opto-prop-2 (4) and (*S*)-Opto-prop-2 (3) were obtained in sufficient amounts and purity for both photochemical and pharmacological evaluations. Optical identity and purity were secured by optical rotation and chiral LC analysis, respectively.

In the dark, the *trans* isomers of (*R*)-Opto-prop-2 (Fig. 1A) and (*S*)-Opto-prop-2 (Fig. 1B) were investigated by UV–Vis absorption spectroscopy in HBSS with 1 % DMSO revealing, as expected, for both enantiomers a λ_{\max} value of 322 nm for their π - π^* transition (Table 1).

Upon illumination with 360 nm the absorbance spectra indicate photoisomerization to the *cis* isomers with a λ_{\max} value of 425 nm for their n - π^* transition. A photostationary state (PSS) containing over 85 % *cis* isomer can be reached upon continuous illumination with 360 nm for both *S*- or *R*-enantiomers. Following thermal relaxation experiments at 60–80 °C, the half-lives of PSS_{*cis*} state at room temperature for both enantiomers extrapolated to be more than ten days (Table 1). Subsequent illumination with 434 nm light back-switched both enantiomers from the PSS_{*cis*} to the PSS_{*trans*} state (Table 1; Fig. 1A and B). As expected, both enantiomers are identical in terms of half-life and PSS values (Fig. 1C and D, Table 1). Dynamic photoisomerization by alternating illumination at 360 and 430 nm showed that for both azobenzene analogs the isomerization is quick, reversible and can be repeated several times. (Fig. 1E and F).

3.2. Characterization of the binding of (*S*)-Opto-prop-2 enantiomers to β ARs

Racemic Opto-prop-2 (VUF17062) was previously shown to act as a *cis*-on antagonist on both β_1 AR and β_2 AR with approximately 25- and 600-fold increase in binding affinity, respectively, upon photoswitching from *trans*- into PSS_{*cis*} isomer (Table 2) [12]. Moreover, PSS_{*cis*} Opto-prop-2 displayed 80-fold selectivity for β_2 AR over β_1 AR, whereas only a 3-fold difference in selectivity was observed for the *trans* isomer. Competition [³H] DHA binding assays revealed that *trans*- and PSS_{*cis*}-isomers of the (*S*)-Opto-prop-2 enantiomer display comparable binding affinities and consequently photoaffinity shift for both β_1 AR (Δ pK_i = 1.4,

25-fold) and β_2 AR (Δ pK_i = 3.0, 1000-fold) as observed for the racemic Opto-prop-2 (Fig. 2A and B, Table 2). The *trans*-isomer of (*R*)-Opto-prop-2 enantiomer shows a similar affinity for β_1 AR but shows no affinity increase (Δ pK_i = 0.2, 2.0-fold) upon photoswitching into the PSS_{*cis*} (Fig. 2C, Table 2). Besides, the (*R*)-Opto-prop-2 enantiomer exhibited lower binding affinity and photoaffinity shift (Δ pK_i = 2.1, 126-fold, Fig. 2D) for β_2 AR compared to racemic Opto-prop-2 (Δ pK_i = 2.8, 630-fold).

Following these studies, we selected (*S*)-Opto-prop-2 as the best photoswitchable tool for the study of β_2 AR. To rationalize the observed 1000-fold affinity difference between the *trans* and PSS_{*cis*} of (*S*)-Opto-prop-2 for β_2 AR, we predicted their binding poses by *in silico* docking using the crystal structure (PDB ID: 6PS5) of inactive β_2 AR in complex with propranolol [18]. The hydroxyl substituent of propranolol engages in polar interactions with D113^{3.32} and N312^{7.39} in the amine pocket, whereas its naphthalene moiety forms hydrophobic/aromatic interactions with F193^{ECL2}, Y199^{5.38}, F289^{6.51} and F290^{6.52} in the extracellular vestibule and major pocket (Fig. 3A). Both *trans* and *cis* photoisomers of (*S*)-Opto-prop-2 are predicted to bind in a comparable orientation as propranolol with their hydroxyl substituent moiety interacting with D113^{3.32} and N312^{7.39} (Fig. 3B and C). The sidechain of the *cis* photoisomer aligns well with the sidechain of propranolol and its azobenzene moiety is accommodated by the hydrophobic pocket for the naphthalene rings of propranolol (Fig. 3B). However, the *trans* azobenzene configuration prevents its binding deep into this pocket, leading to apparently less optimal interaction of the lower azobenzene ring with the aromatic sidechains and the hydroxyl substituent with D113^{3.32}

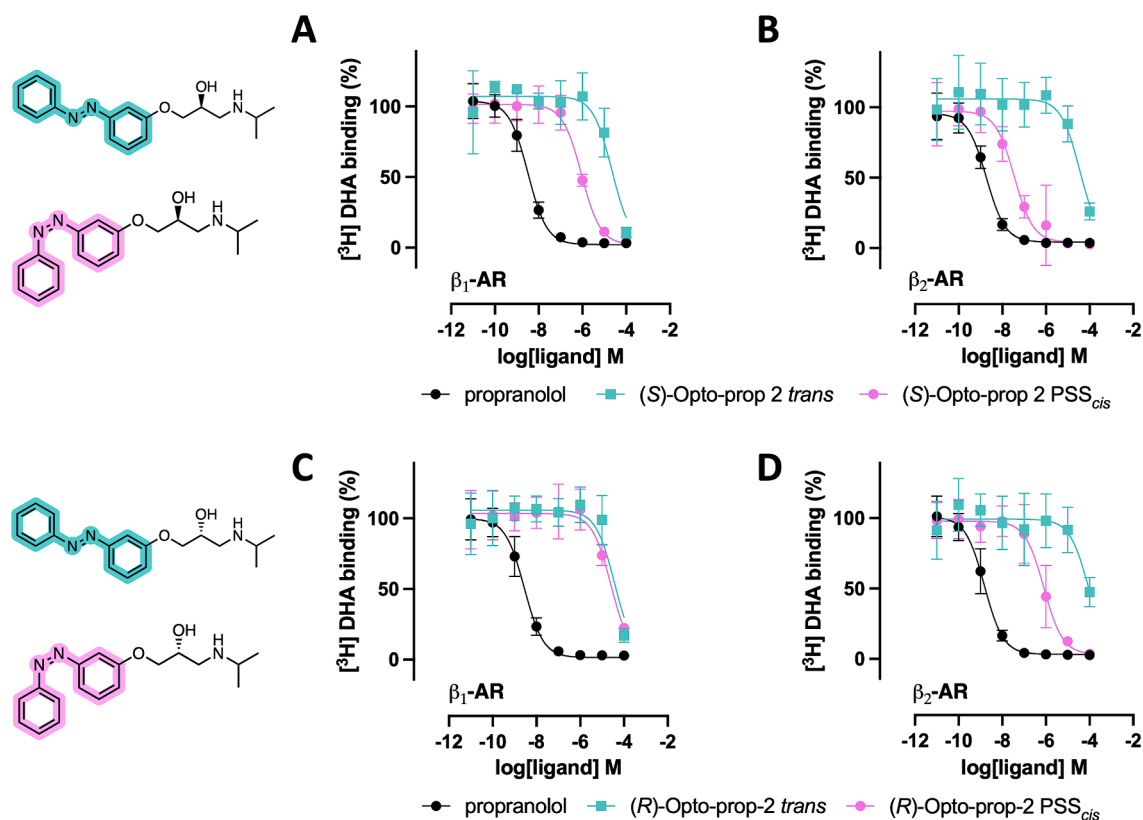


Fig. 2. Binding of photoswitchable Opto-prop-2 *S*- and *R*-enantiomers to β_1 AR and β_2 AR. Competition of [³H] DHA binding to HEK293T membranes expressing the β_1 AR (A, C) or β_2 AR (B, D) by photoswitchable (*S*)-Opto-prop-2 (A, B) and (*R*)-Opto-prop-2 (C, D) without prior illumination (i.e. *trans* depicted in cyan) and pre-illuminated with 360 nm light (i.e. PSS_{cis} depicted in magenta). Propranolol (with black circles) is depicted in all graphs as a reference compound. Data are shown as the mean \pm SD of ≥ 3 independent experiments in triplicates.

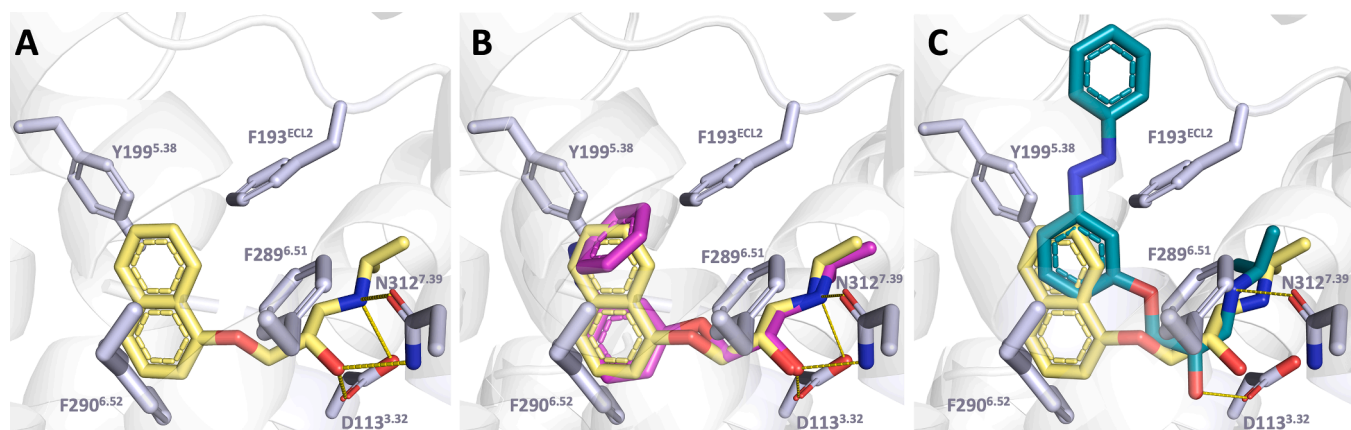


Fig. 3. Predicted binding poses of photoswitchable (*S*)-Opto-prop-2 in complex with the β_2 AR. The structure of the β_2 AR co-crystallized beta-blocker propranolol (yellow; PDB ID: 6PSS) (A) was used to superimpose the predicted binding pose of (*S*)-Opto-prop-2 *cis* depicted in magenta (B) and the predicted binding pose of (*S*)-Opto-prop-2 *trans* depicted in cyan (C). Polar interactions are indicated with yellow lines.

and N312^{7.39} (Fig. 3C).

To validate the predicted binding poses, site-directed mutagenesis was performed to evaluate the contribution of individual amino acids in ligand binding. In line with earlier findings, the glutamic acid substitution of D113^{3.32} impairs [³H] DHA binding and could consequently not be further analyzed for propranolol and (*S*)- and (*R*)-Opto-prop-2 competition binding [23]. The β_2 AR mutants F193^{ECL2}A, Y199^{5.38}A, F289^{6.51}A, F290^{6.52}A and N312^{7.39}Q are expressed at 1.7- to 13.8-fold lower B_{max} levels and displayed 4- to 100-fold lower binding affinities for [³H] DHA as compared to wild type β_2 AR (Fig. 4 and Table 3).

In line with the observed binding pose in the crystal structure of propranolol bound to β_2 AR (Fig. 3A) [18], all generated mutant receptors displayed significantly decreased binding affinities for propranolol (Table 3), confirming that these amino acids are involved in polar or hydrophobic interaction with propranolol. In particular, Ala substitution of F289^{6.51} resulted in a 200-fold reduced binding affinity for propranolol, whereas 10- to 50-fold reduced affinities were observed for F193^{ECL2}A, Y199^{5.38}A, F290^{6.52}A and N312^{7.39}Q (Fig. 4A, B, D, E and Table 3). The F289^{6.51}A mutation also reduced the high affinity of (*S*)-Opto-prop-2 PSS_{cis} by 200-fold, whereas the low affinity of (*S*)-Opto-

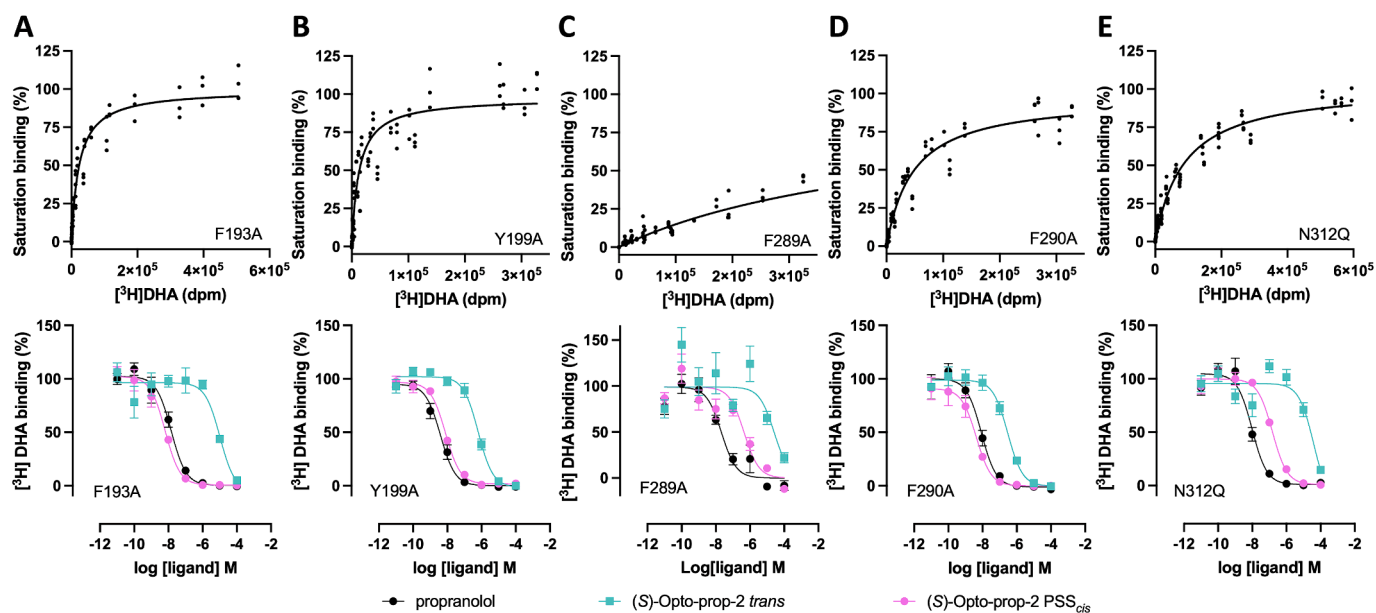


Fig. 4. Saturation and competition binding assay for mutant β_2 AR. (A-E) upper panel, saturation binding assay for mutant β_2 AR; (A-E) lower panel, competition binding assay for β_2 AR. The binding assays were performed using [3 H] DHA with membranes expressing WT or mutant β_2 AR. Data are plotted for at least three independent experiments and represented mean \pm SD values of pooled experiments.

Table 3

Binding affinities for reference antagonists and (S)-Opto-prop-2 isomers for WT and mutant β_2 AR.

β_2 AR	$pK_d^{[a]}$	$pK_i^{[b]}$ for the unlabeled ligands			B_{max} pmol/mg
	[3 H] DHA	propranolol ^[b]	(S)-Opto- prop-2 ^[b] <i>trans</i>	(S)-Opto- prop-2 ^[b] <i>PSS_{cis}</i>	
WT	9.6 \pm 0.2 (4)	9.8 \pm 0.1 (8)	5.5 \pm 0.1 (4)	8.5 \pm 0.2 (4)	33.0 \pm 19 (4)
D113 ^{3,32E}	N/A	N/A	N/A	N/A	N/A
F193 ^{ECL2A}	9.0 \pm 0.3 (3) [4.0] **	8.1 \pm 0.2 (3) [50] ****	5.5 \pm 0.2 (3)[1.0]	8.7 \pm 0.2 (3)[1.6]	19.3 \pm 3.7 (3) [1.7]
Y199 ^{5,38A}	9.2 \pm 0.4 (4) [2.5] *	8.8 \pm 0.4 (3) [10] ****	6.7 \pm 0.3 (4) [16] ****	8.6 \pm 0.0 (4)[1.3]	5.0 \pm 1.3 (4) [6.6] ***
F289 ^{6,51A}	7.6 \pm 0.1 (4) [100] ****	7.5 \pm 0.1 (4) [200] ****	4.6 \pm 0.3 (4) [8.0] ***	6.2 \pm 0.4 (4) [200] ****	2.4 \pm 0.5 (4) [13.8] ***
F290 ^{6,52A}	8.7 \pm 0.2 (4) [10] ****	8.2 \pm 0.3 (3) [40] ****	6.8 \pm 0.2 (4) [20] ****	8.7 \pm 0.2 (4)[1.6]	16.2 \pm 4.1 (4) [2] *
N312 ^{7,39Q}	8.5 \pm 0.2 (5) [13] ****	8.2 \pm 0.2 (3) [40] ****	4.8 \pm 0.1 (4) [5] ***	7.0 \pm 0.2 (5) [31] ****	13.3 \pm 4.3 (5) [2.5] *

[a] the binding affinity (pK_d) of [3 H] DHA was determined by saturation binding of increasing concentrations [3 H] DHA to HEK293T membranes expressing WT or mutant β_2 AR in the absence and presence of 10 μ M propranolol quantify non-specific binding. [b] the binding affinity (pK_i) of unlabelled compounds was determined by radioligand competition binding. Fold decrease (\downarrow) or increase (\uparrow) in binding affinity and B_{max} value compared to WT β_2 AR is indicated between brackets. Data are shown as the mean \pm SD of ≥ 3 independent experiments (indicated between parentheses) performed in triplicate. Statistic differences between WT and mutant pK_i values were analyzed with a One-way ANOVA test under Dunnett's multiple comparisons, p-values as follows: *p = 0.03 **p = 0.002 ***p = 0.0002 ****p < 0.0001, N/A = not available.

prop-2 *trans* is 8-fold further reduced (Fig. 4C and Table 3).

In addition, N312^{7,39Q} reduced the binding affinity of both (S)-Opto-prop-2 *PSS_{cis}* and *trans* isomers by 31- and 5-fold, respectively, confirming its importance for the binding of (S)-Opto-prop-2 *PSS_{cis}* and similar to other β AR ligands [24]. In contrast to propranolol, the binding affinity of (S)-Opto-prop-2 *PSS_{cis}* was not significantly affected by the F193^{ECL2A}, Y199^{5,38A}, and F290^{6,52A} mutations, suggesting that the bent *cis* azobenzene moiety fits well in this hydrophobic pocket, but in contrast to the naphthalene moiety of propranolol is not significantly engaged in hydrophobic interactions with these residues. Moreover, the replacement of the bulky aromatic side chains of Y199^{5,38A} and F290^{6,52A} with a small methyl sidechain (Ala) increased the affinity of (S)-Opto-prop-2 *trans* by 16- and 20-fold, respectively. Based on these data we suggest that in the WT β_2 AR the elongated *trans* azobenzene clashes with Y199^{5,38A} and F290^{6,52A} residues. Consequently, this hampers the important interactions of the ethanolamine moiety of (S)-Opto-prop-2 *trans* with D113^{3,32E} and N312^{7,39Q}.

Finally, the binding of the (S)-Opto-prop-2 enantiomers to β_2 AR was studied with confocal microscopy (Fig. 5). To this end, N-terminal SNAP-tagged β_2 AR were labelled with green-fluorescent sSNAP-AF488 on the surface of intact HEK293T cells (Fig. 5B, top row). Following incubation with 10 nM of a red fluorescent derivative of antagonist ICI,118–551, its membrane binding could also be detected on the surface of intact HEK293T cells (Fig. 5B, middle row). Under control conditions, the red fluorescence colocalizes with sSNAP-labelled β_2 AR on the cell surface (Fig. 5B, merged channel). The binding of the fluorescent ligand was significantly reduced in the presence of 1 μ M pre-illuminated *PSS_{cis}* (S)-Opto-prop-2, as compared to the buffer control (ctrl) (Fig. 5B and C). In line with the results from [3 H] DHA binding assay, 1 μ M of *trans* (S)-Opto-prop-2 displayed only a negligible effect on fluorescent ICI,118–551 binding (Fig. 5B and C). However, *in situ* illumination of *trans* (S)-Opto-prop-2 with 385 nm for 3 min reduced binding of fluorescent ICI,118–551 to a similar extent as when pre-illuminated *PSS_{cis}* (S)-Opto-prop-2 was used (Fig. 5B and C), indicating that low-affinity *trans*-isomer can be successfully switched to the high-affinity *cis*-isomer on living cells.

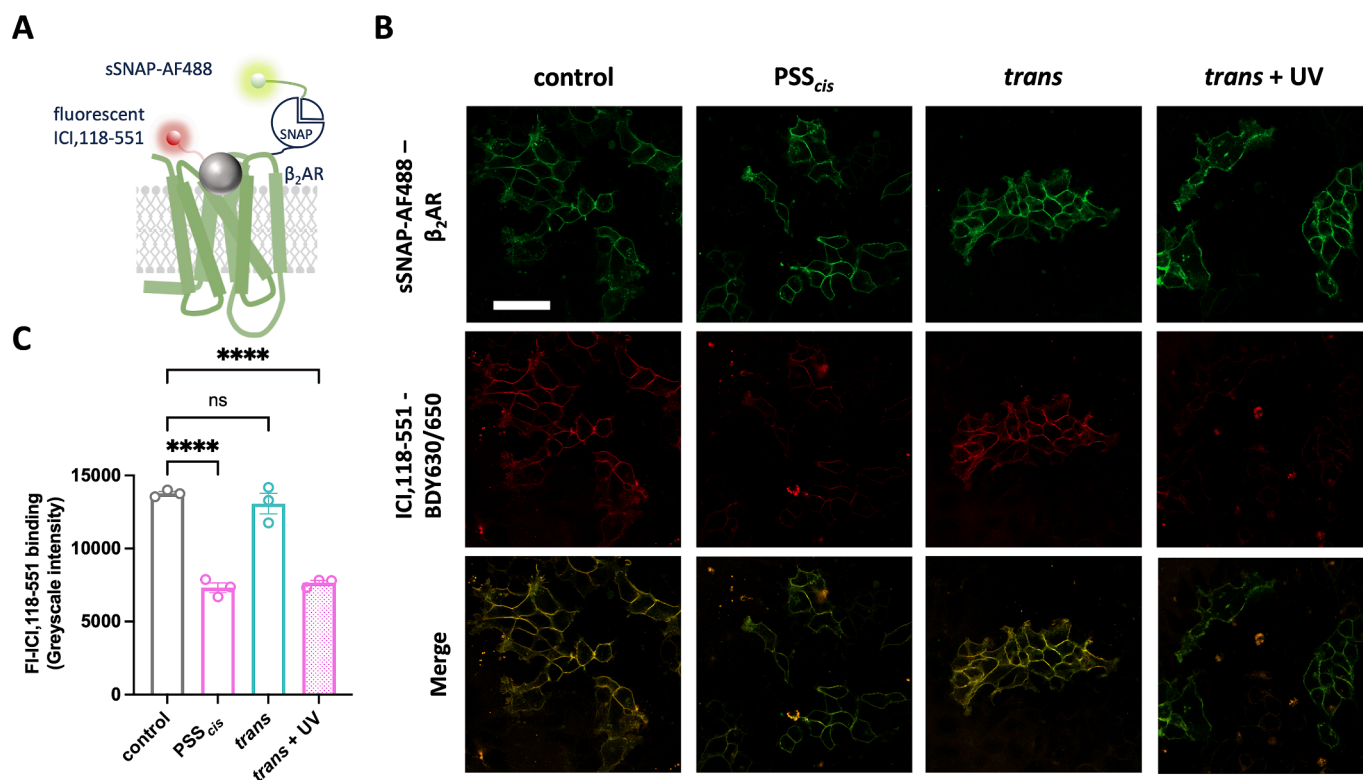


Fig. 5. Optical control of (S)-Opto-prop-2 binding to β_2 AR. (A) The illustration of the interaction between SNAP-tagged β_2 AR and fluorescent ICI,118-551. (B) Confocal imaging of sSNAP-AF488 labelling (top panel) and fluorescent ICI,118-551 binding (middle panel) to sSNAP-tagged β_2 AR in HEK293T cells pre-incubated for 30 min with buffer (control), 1 μ M PSS_{cis} or *trans* of (S)-Opto-prop-2. Merged channels are shown in the bottom panel, where yellow indicates co-localised pixels. Wells under UV conditions were exposed to 385 nm LED for 3 min before the addition of 10 nM fluorescent ICI,118-551. The scale bar represents 50 μ m. (C) Fluorescent ICI,118-551 (BDY-630/650) intensity as determined by membrane regions of interest. Data are mean \pm SEM of three independent experiments performed in triplicate. One-way ANOVA was performed with Dunnett's multiple comparison test; **** $p < 0.0001$.

3.3. *In vitro* and *in vivo* evaluation of (S)-Opto-prop-2 enantiomers as β_2 AR antagonists

A FRET-based EPAC cAMP and NanoBiT-based β -arrestin2 recruitment assays were used to functionally evaluate the photoisomers of (S)- and (R)-Opto-prop-2 as β_2 AR antagonists. Isoprenaline increases cAMP levels in HEK293 cells via endogenously expressed β_2 AR with a pEC₅₀ value of 8.5 ± 0.3 (Fig. 6A), as measured with a stably expressed FRET-based EPAC sensor. In transiently transfected HEK293T-cells, LgBiT- β -arrestin2 recruitment to co-transfected β_2 AR-SmBiT was induced by isoprenaline with a pEC₅₀ value of 8.0 ± 0.1 (Fig. 6D). Similar to propranolol, both the (S)- and (R)-Opto-prop-2 enantiomers antagonize isoprenaline-induced (at EC₈₀ concentration) cAMP production (Fig. 6B and C) and β -arrestin2.

recruitment (Fig. 6E and F). Both (S)- and (R)-Optoprop-2 act as *cis*-on antagonists with pK_b values and photo-induced pK_b shift values (Δ pK_b) between their dark *trans* and pre-illuminated PSS_{cis} that are comparable to those observed in competition binding experiments (Table 4). Indeed, with a 398-fold increase in pK_b value upon the illumination with 360 nm, (S)-Opto-prop-2 is a clearly more potent photoswitchable β -blocker as compared to (R)-Opto-prop-2.

Beta-blockers are clinically used to reduce ocular hypertension by antagonizing β AR-mediated aqueous humor production in the eye [25,26]. Transient ocular hypertension (OHT) in the rabbit eye was triggered by injecting hypertonic saline (5%) into the vitreous and the intraocular pressure for all the set-ups reached between 35 to 40 mmHg upon 10 mins. Antagonists were administered as eye-drop immediately following the stimulation of IOP (Fig. 7A). The treatment with either 0.1% propranolol or pre-illuminated PSS_{cis} (S)-Opto-prop-2 significantly reduced the intraocular pressure at 60 min (-2.7 ± 1.2 mmHg, $p <$

0.05), whereas the same dose of the low affinity (S)-Opto-prop-2 *trans* was ineffective (Fig. 7C). In line with our *in vitro* data, the PSS_{cis} also acts *in vivo* as a high-affinity antagonist with a comparable effect as propranolol at the tested concentration, whereas the low-affinity *trans* isomer is ineffective.

3.4. Dynamic and reversible modulation of β_2 AR with (S)-Opto-prop-2 photoswitch

Finally, dynamic modulation of agonist-induced β_2 AR signaling by alternating *in situ* photoswitching of (S)-Opto-prop-2 between *trans* and *cis* isomers using LED-array plates was measured by a FRET-based EPAC sensor to measure cAMP levels in a microplate reader (Fig. 8A). Pre-incubation of cells in the dark with 24 nM isoprenaline (EC₉₀ concentration) in combination with 10 nM of the low-affinity (S)-Opto-prop-2 *trans* isomer for 45 min resulted in 90% cAMP production (Fig. 8B). Illumination of these cells using a 365 nm LED array plate for 10 min to switch (S)-Opto-prop-2 *trans* into the high-affinity *cis* isomer at PSS_{cis} reduced cAMP production to 25%, i.e. resulted in more efficiently antagonizing isoprenaline-induced β_2 AR activity (Fig. 8B).

Subsequent illumination using a 430 nm LED array plate relieves (S)-Opto-prop-2-mediated antagonism of isoprenaline signaling by switching the high-affinity *cis* isomer back into the low-affinity *trans* isomer. Alternating illumination with these LED array plates confirmed that photoswitching is reversible over multiple cycles and allowed accurate *in situ* control of antagonizing the isoprenaline-induced β_2 AR activity. In addition, to avoid overlap with the wavelengths for photoswitching of (S)-Opto-prop-2, the dynamic modulation experiment was also measured using the Red cADDIS™ cAMP sensor with red-shifted excitation and emission wavelengths. Comparable reversible light-

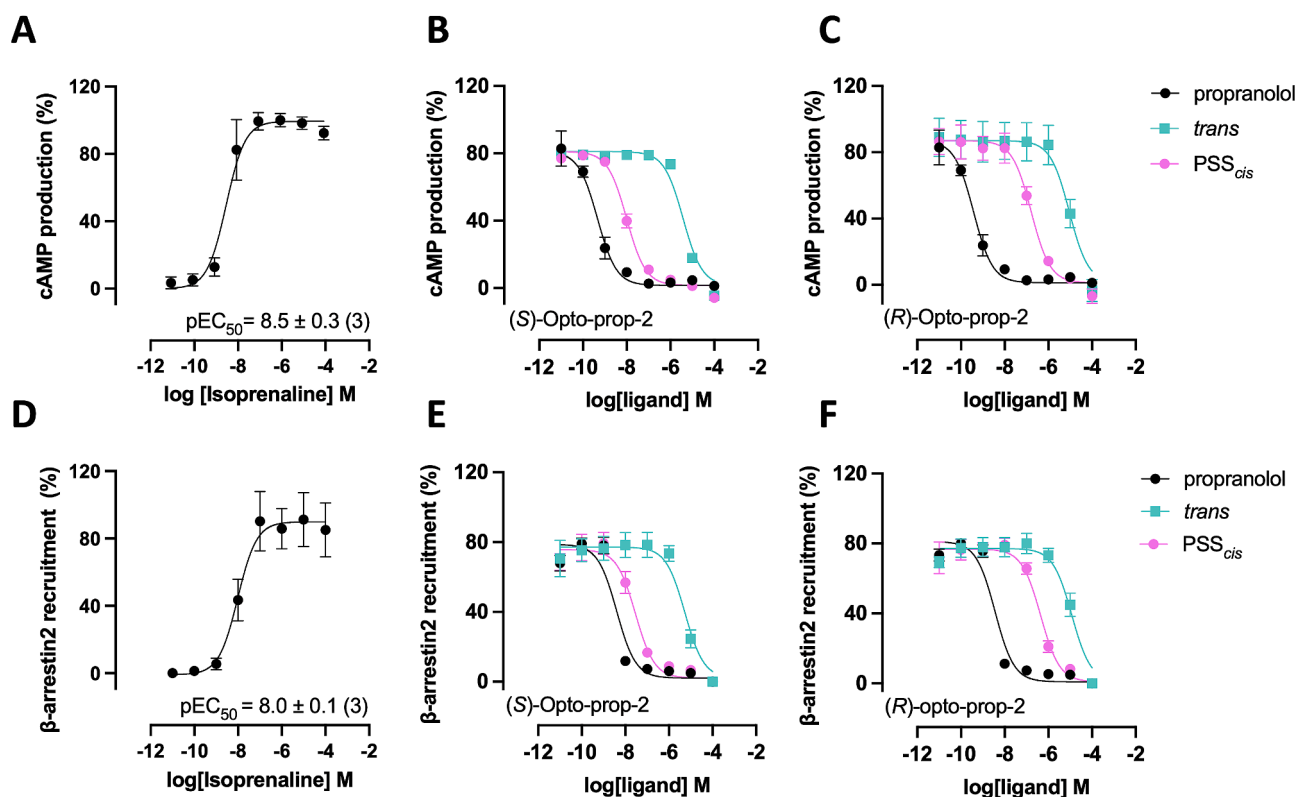


Fig. 6. Antagonism of β_2 AR activity by photoswitchable-propranolol S- and R-enantiomers. β_2 AR induced cAMP production (A) and β -arrestin2 recruitment (D) in response to isoprenaline stimulation were detected by FRET-based EPAC sensor (A, B and C) and NanoBiT (D, E and F) assays, respectively and antagonized by (S)-Opto-prop-2 (B, E) or (R)-Opto-prop-2 (C, F) without (*trans* in cyan) or with pre-illumination at 360 nm (PSS_{cis} in magenta). Reference antagonist propranolol is depicted in black. Data are shown as the mean \pm SD of ≥ 3 independent experiments in triplicates.

Table 4

Functional characterization of photoswitchable-propranolol S- and R-enantiomer on the β_2 AR.

Compound	cAMP production			β -arrestin2 recruitment		
	pK_b <i>trans</i> ^[a]	pK_b PSS _{cis} ^[b]	ΔpK_b ^[c]	pK_b <i>trans</i>	pK_b PSS _{cis}	ΔpK_b
propranolol	10.1 \pm 0.2 (4)	N/A	N/A	9.2 \pm 0.0 (9)	N/A	N/A
(S)-Opto-prop-2 (VUF25474)	6.1 \pm 0.0 (3)	8.7 \pm 0.1 (3)	2.6 \pm 0.1	5.9 \pm 0.1 (3)	8.4 \pm 0.1 (3)	2.4 \pm 0.2
(R)-Opto-prop-2 (VUF25475)	5.7 \pm 0.2 (3)	7.4 \pm 0.2 (3)	1.7 \pm 0.1	5.5 \pm 0.1 (3)	7.1 \pm 0.1 (3)	1.7 \pm 0.0

^[a] compounds were left in the dark during the whole experimental procedure. ^[b] compounds were pre-illuminated under 360 nm to PSS_{cis} before experimentation. ^[c] pK_b was determined from IC₅₀ values following the Cheng-Prusoff correction. Data represented the difference between the pK_b of *trans* compared to PSS_{cis}. All the values are expressed as mean \pm SD of ≥ 3 experiments performed in triplicates. N/A = not applicable.

modulation of β_2 AR-mediated cAMP signaling by (S)-Opto-prop-2 was measured using HEK293T that transiently expresses the red fluorescence intensity-based cAMP sensor cADDisTM (Fig. 8C). These orthogonal assays show that dynamic and reversible modulation of β_2 AR function can be realized by photoswitching of (S)-Opto-prop-2.

4. Discussion

Photoswitchable ligands for GPCRs offer the promise of dynamic spatiotemporal control of GPCR action and ultimately improved therapeutic windows [1,27,28]. With the development of azobenzene-derived GPCR ligands, a fair number of GPCR photoswitchable tools have been developed for both family A [1] and family C GPCRs [3]. So far, a photoswitch with one of the largest differences in *trans* and *cis* affinity has been Opto-prop-2, the azobenzene analog of propranolol [12]. Propranolol, originally discovered as beta-blocker by Sir James Black and colleagues and developed as the first live-saving drug for angina pectoris [29], was used as template for a simple, but effective azologization strategy [1,12]. The replacement of the naphthalene

moiety of propranolol with an azobenzene group, connected with the oxypropanolamine sidechain at the *meta* position, yielded the *cis*-active photoswitchable β_2 AR antagonist Opto-prop-2 (VUF17062) with an almost 600-fold increased binding affinity upon illumination at 360 nm [12].

Since Opto-prop-2 was racemic, in this study, we synthesized and characterized the S- and R- enantiomer of Opto-prop-2. Both enantiomers could be obtained in good yield and purity. As expected, in the dark (i.e. *trans*-configuration) both (S)- and (R)-Opto-prop-2 were almost inactive at both tested β ARs (Table 2). Both enantiomers effectively (>90 %) switch within seconds into the *cis*-configuration after 360 nm illumination and can be easily switched back with 430 nm illumination. In fact, as observed often for plain azobenzene-derived photoswitches [1] thermodynamic back-switching of the *cis*-configuration is very slow at 20 °C (half-life > 10 days, Table 1) and spontaneous back-switching could only be observed upon heating. At PSS_{cis} both (S)- and (R)-Opto-prop-2 were binding best at β_2 AR, with (S)-Opto-prop-2 being the best *cis*-on photoswitch with 3 nM affinity and a 1000-fold gain in affinity upon azobenzene switching (Table 2). These photopharmacology

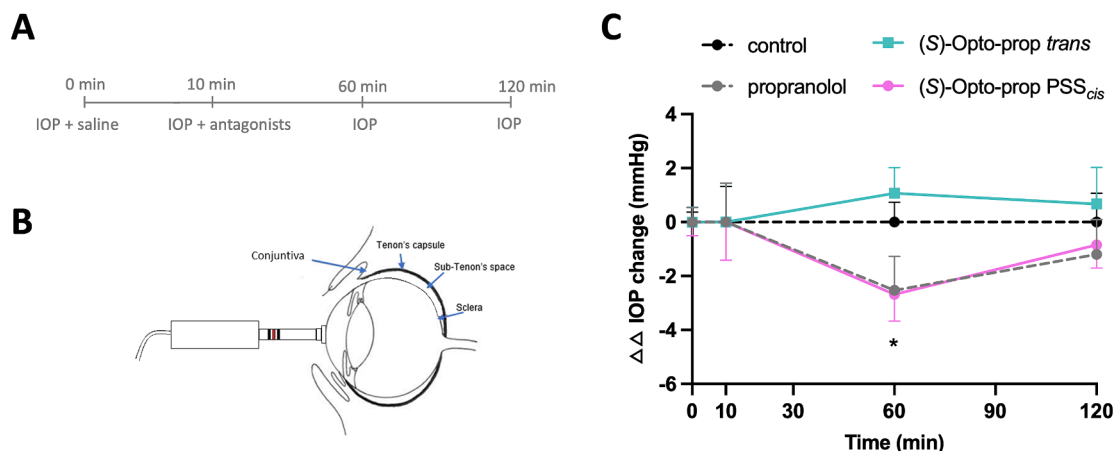


Fig. 7. Effect of photoswitchable antagonist (S)-Opto-prop-2 on intraocular pressure (IOP) in rabbits. (A) Schematic time scheme for the generation of Transient ocular hypertension (OHT) model and the application of photoswitchable antagonists (B) Illustration of IOP measurement (C) Time course of IOP changing upon the addition of the ligand. * $p < 0.05$ for (S)-Opto-prop-2 PSS_{cis} versus *trans* state at 60 min. Results were analysed with the mean \pm SEM with an unpaired *t*-test. $n = 22$ for the control group, $n = 9$ for propranolol, $n = 17$ for *trans* isomer and $n = 15$ for PSS_{cis} isomer.

properties make (S)-Opto-prop-2 one of the best reported GPCR photoswitches so far.

The observed high affinity of *cis*-(S)-Opto-prop-2 is perfectly aligned with the well-known stereospecificity of ligand binding to β_2 AR [30]. Importantly, the molecular docking of *trans*- and *cis*-(S)-Opto-prop-2 in the propranolol-bound x-ray structure of the β_2 AR (PDB ID: 6PS5) [18] indicate that the *cis* azobenzene configuration allows (S)-Opto-prop-2 to align well with the experimentally determined binding mode of propranolol. Especially, the oxypropanolamine sidechain of *cis*-(S)-Opto-prop-2 shows a perfect overlay with the propranolol sidechain, making effective interactions with D113^{3.32} and N312^{7.39}. Both residues are known to be crucial for effective interaction with aminergic ligands [23,24,31] and their key role in binding was confirmed by site-directed mutagenesis in this study. In the observed docking pose for the *trans*-configuration its sidechain cannot perfectly interact with both D113^{3.32} and N312^{7.39}. This suggestion is substantiated by the relatively small loss in binding following mutagenesis of N312^{7.39}. Also, in the best docking pose the elongated azobenzene moiety of *trans*-(S)-Opto-prop-2 sticks out of the binding pocket. Since alanine substitution of Y199^{5.38} and F290^{6.52} enhances the affinity of the *trans*-configuration 12- and 16-fold respectively, these mutants most likely decrease a steric hinderance between the *trans*-azobenzene rings and surrounding aromatic residues in the top of the transmembrane regions.

Based on the *in vitro* data, (S)-Opto-prop-2 is a new chemical biology tool for the spatiotemporal modulation of β_2 AR, as e.g. also shown by the microscopy-based modulation of the binding of the fluorescent-labeled ICI,118–551. This ligand is a well-known selective β_2 AR antagonist [32] and a fluorescent BODIPY-analog was recently reported to label β_2 AR in transfected cells at low expression levels [17]. In confocal imaging experiments, binding of the BODIPY-labelled ICI,118–551 analog to SNAP-tagged β_2 AR could also be shown in this study. The fluorescent labelling of β_2 AR could be prevented by coinubation with 1 μ M of PSS_{cis} (S)-Opto-prop-2, but not with *trans*-(S)-Opto-prop-2. Yet, *in situ* switching of *trans*-(S)-Opto-prop-2 to its active *cis*-variant led to the expected displacement of BODIPY-ICI,118–551 binding. In the various functional assays (cAMP production, β -arrestin2 recruitment), (S)-Opto-prop-2 showed clear antagonism of β_2 AR stimulation, with again a strong preference for the *cis*-form. This was not only observed with preilluminated samples, but was also observed in a dynamic setup, where *in situ* (S)-Opto-prop-2 was repetitively illuminated with either 360 or 430 nm. The levels of cAMP were measured with 2 orthogonal assays, i. e. an EPAC-based sensor [21] and the Red cADDISTM assay system [33] to exclude potential interference of the assay with the *in situ* photoswitching of (S)-Opto-prop-2. The data obtained in both assay systems

indicate that optical modulation of (S)-Opto-prop-2 leads to dynamic modulation of β_2 AR activation.

Beta blockers find a number of therapeutic applications, including glaucoma [8]. Glaucoma results in progressive ocular neuropathy and is often associated with high intraocular pressure (IOP) [34]. Beta-blockers are well-known to reduce aqueous humour production and decrease IOP in humans [25,26]. In this study, we used an established model to measure IOP in New Zealand white rabbits [20,26] and investigate the effect of the photoswitchable (S)-Opto-prop-2 *in vivo*. In line with *in vitro* experiments, also *in vivo* the *cis*-isomer of (S)-Opto-prop-2 behaves similarly to propranolol, whereas the low-affinity *trans*-isomer did not affect the IOP in the tested animals.

In conclusion, in this study we present (S)-Opto-prop-2, a high affinity, *cis*-on β_2 AR photoswitch, exhibiting a 1000-fold difference in binding affinity for β_2 AR upon photoswitching of its inactive *trans*-form. This makes (S)-Opto-prop-2 one of the best photoswitchable GPCR ligands, reported so far. Molecular modelling combined with site-directed mutagenesis provides a structural basis for the observed optical modulation. Furthermore, β_2 AR signaling can be modulated dynamically and reversibly using the (S)-Opto-prop-2 both *in vitro* and *in vivo*. This new tool will allow future studies of spatiotemporal signalling by β_2 AR. Moreover, the present scaffold also offers a promising lead for the development of next generation photoswitchable β -blockers with e.g. improved photochemical properties. For ultimate *in vivo* application of photoswitchable molecules, one should preferably move away from illumination in the UV-spectrum and develop so-called red-shifted photoswitchable ligands, i.e. ligands with substituted azobenzene groups [35–37] or completely different photoswitchable moieties [38,39]. For certain applications, i.e. modulation of heart function with photoswitches, similar to a recent report on rats with local optogenetic targeting and LED implantation, also the actual thermodynamic half-life of the *cis*-active ligands might be an important parameter to modulate [40].

CRedit authorship contribution statement

Shuang Shi: Writing – original draft, Validation, Methodology, Investigation, Funding acquisition, Formal analysis. **Yang Zheng:** Writing – original draft, Methodology, Investigation, Formal analysis. **Joëlle Goulding:** Writing – original draft, Methodology, Investigation, Formal analysis. **Silvia Marri:** Methodology, Investigation, Formal analysis. **Laura Lucarini:** Methodology, Investigation, Formal analysis. **Benjamin Konecny:** Methodology, Formal analysis. **Silvia Sgambellone:** Methodology, Investigation, Formal analysis. **Serafina Villano:**

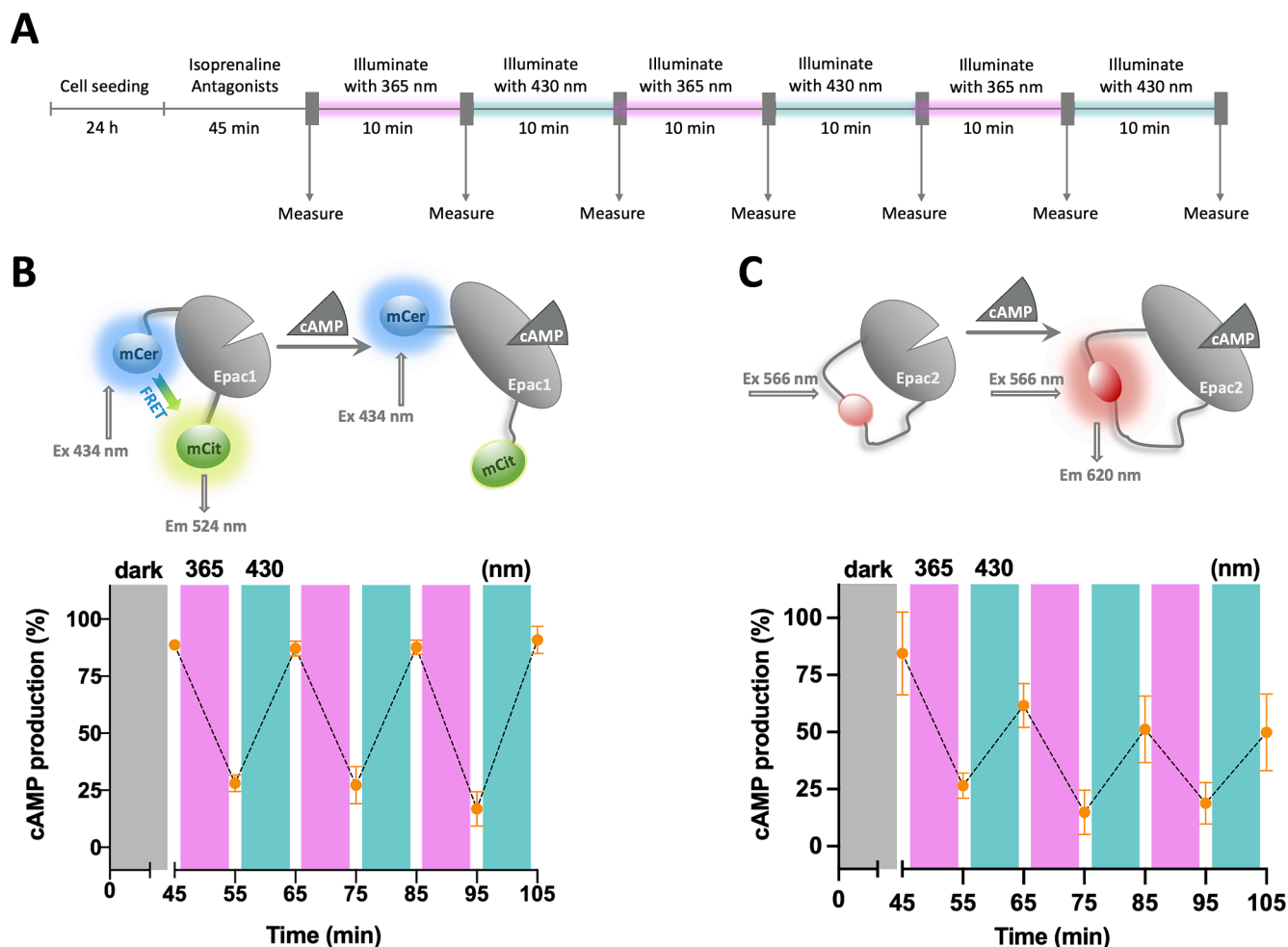


Fig. 8. Dynamic and reversible modulation of β_2 AR by photoswitchable antagonist (*S*)-Opto-prop-2. (A) Schematic time scheme for dynamic modulation of β_2 AR activity in a microplate reader (B) The illustration of FRET-based EPAC-sensor (upper panel). mCerulean (mCer) and mCitrine (mCit) were fused on each side of Epac1. Binding of cAMP changes Epac1 conformation resulting in a reduced Förster resonance energy transfer (FRET) between mCer and mCit. Detection of cAMP levels in HEK293 cells upon 45 min pre-incubation in the dark with 24 nM isoprenaline and 10 nM (*S*)-Opto-prop-2 *trans* and following subsequent alternating illumination with 365 nm (magenta) and 430 nm (cyan) wavelengths for 10 min to photoswitch between *cis* and *trans*, respectively (bottom panel). (C) Cartoon of the Red cADDISTM cAMP sensor (upper panel). The circularly permuted red-fluorescent protein was fused to Epac2. Binding of cAMP-induced the change in the conformation of Epac2 and further increased red fluorescence. The time-trace intracellular cAMP change was monitored using an FI-based cADDISTM cAMP assay (bottom panel). HEK293T cells were incubated with 0.3 nM isoprenaline and (*S*)-Opto-prop-2 *trans* in the dark before illumination with 365 nm (magenta) and 430 nm (cyan) for 10 min respectively. Data were shown as mean \pm SD with three individual experiments.

Methodology, Formal analysis. **Reggie Bosma:** Writing – review & editing, Supervision, Methodology, Investigation, Formal analysis. **Maikel Wijtmans:** Writing – review & editing, Supervision, Resources, Project administration, Methodology, Conceptualization. **Stephen J. Briddon:** Writing – review & editing, Supervision, Methodology. **Barbara A. Zarzycka:** Writing – review & editing, Methodology. **Henry F. Vischer:** Writing – review & editing, Supervision, Resources, Project administration, Methodology, Conceptualization. **Rob Leurs:** Writing – review & editing, Supervision, Resources, Project administration, Methodology, Conceptualization.

Declaration of competing interest

The authors declare that they have no known competing financial interests or personal relationships that could have appeared to influence the work reported in this paper.

Data availability

Data will be made available on request.

Acknowledgments

This work was supported by FLAG-ERA funding HA-CTion (NWO 680-91-316) to YZ and RL. SS acknowledges the China Scholarship Council (CSC) for funding (Grant No.202006310016). The authors thank Prof. Emanuela Masini for the careful revision of the manuscript. Anne Marie Quinn from Montana Molecular for helpful discussion and providing Red upward-cADDISTM cAMP biosensor. Hans Custers, Andrea van de Stolpe and Elwin Janssen are acknowledged for assistance and advice.

References

- [1] M. Wijtmans, I. Josimovic, H.F. Vischer, R. Leurs, Optical control of Class A G protein-coupled receptors with photoswitchable ligands, *Curr. Opin. Pharmacol.* 63 (2022) 102192, <https://doi.org/10.1016/j.coph.2022.102192>.
- [2] M.J. Fuchter, On the Promise of Photopharmacology Using Photoswitches: A Medicinal Chemist's Perspective, *J. Med. Chem.* 63 (2020) 11436–11447, <https://doi.org/10.1021/acs.jmedchem.0c00629>.
- [3] S. Panarello, X. Rovira, A. Llebaria, X. Gómez-Santacana, *Photopharmacology of G Protein-coupled receptors*, *Molecular Photoswitches*, Wiley, in, 2022, pp. 921–944.
- [4] M. Ricart-Ortega, J. Font, A. Llebaria, GPCR photopharmacology, *Mol. Cell. Endocrinol.* 488 (2019) 36–51, <https://doi.org/10.1016/j.mce.2019.03.003>.

- [5] W. Szymański, J.M. Beierle, H.A.V. Kistemaker, W.A. Velema, B.L. Feringa, Reversible photocontrol of biological systems by the incorporation of molecular photoswitches, *Chem. Rev.* 113 (2013) 6114–6178, <https://doi.org/10.1021/cr300179f>.
- [6] R. Santos, O. Ursu, A. Gaulton, A.P. Bento, R.S. Donadi, C.G. Bologa, A. Karlsson, B. Al-Lazikani, A. Hersey, T.I. Oprea, J.P. Overington, A comprehensive map of molecular drug targets, *Nat. Rev. Drug Discov.* 16 (2016) 19–34, <https://doi.org/10.1038/nrd.2016.230>.
- [7] L. Filippi, M. Dal Monte, G. Casini, M. Daniotti, F. Sereni, P. Bagnoli, Infantile hemangiomas, retinopathy of prematurity and cancer: A common pathogenetic role of the β -adrenergic system, *Med. Res. Rev.* 35 (2015) 619–652, <https://doi.org/10.1002/med.21336>.
- [8] A.M.V. Brooks, W.E. Gillies, Ocular β -Blockers in Glaucoma Management, *Drugs Aging* 2 (1992) 208–221, <https://doi.org/10.2165/00002512-199202030-00005>.
- [9] J.G. Baker, S.J. Hill, R.J. Summers, Evolution of β -blockers: From anti-anginal drugs to ligand-directed signalling, *Trends Pharmacol. Sci.* 32 (2011) 227–234, <https://doi.org/10.1016/j.tips.2011.02.010>.
- [10] A. Duran-Corbera, J. Font, M. Faria, E. Prats, M. Consegal, J. Catena, L. Muñoz, D. Raldúa, A. Rodríguez-Sinovas, A. Llebaria, X. Rovira, Caged-carvedilol as a new tool for visible-light photopharmacology of β -adrenoceptors in native tissues, *Iscience* 25 (2022), <https://doi.org/10.1016/j.isci.2022.105128>.
- [11] A. Duran-Corbera, J. Catena, M. Otero-Viñas, A. Llebaria, X. Rovira, Photoswitchable Antagonists for a Precise Spatiotemporal Control of β 2-Adrenoceptors, *J. Med. Chem.* 63 (2020) 8458–8470, <https://doi.org/10.1021/acs.jmedchem.0c00831>.
- [12] R. Bosma, N.C. Dijon, Y. Zheng, H. Schihada, N.J. Hauwert, S. Shi, M. Arimont, R. Riemens, H. Custers, A. van de Stolpe, H.F. Vischer, M. Wijtmans, N.D. Holliday, D.W.D. Kuster, R. Leurs, Optical control of the β 2-adrenergic receptor with opto-prop-2: A cis-active azobenzene analog of propranolol, *Iscience* 25 (2022), <https://doi.org/10.1016/j.isci.2022.104882>.
- [13] Z. Ahmed, A. Siiskonen, M. Virkki, A. Priimagi, Controlling azobenzene photoswitching through combined: Ortho-fluorination and -amination, *Chem. Commun.* 53 (2017) 12520–12523, <https://doi.org/10.1039/c7cc07308a>.
- [14] A. Reyes-Alcaraz, Y.N. Lee, S. Yun, J.I. Hwang, J.Y. Seong, Conformational signatures in β -arrestin2 reveal natural biased agonism at a G-protein-coupled receptor, *Commun Biol* 1 (2018), <https://doi.org/10.1038/s42003-018-0134-3>.
- [15] X. Ma, R. Leurs, H.F. Vischer, NanoLuc-Based Methods to Measure β -Arrestin2 Recruitment to G Protein-Coupled Receptors, in: *Methods in Molecular Biology*, Humana Press Inc., 2021, pp. 233–248, https://doi.org/10.1007/978-1-0716-1221-7_16.
- [16] J. Goulding, A. Kondrashov, S.J. Mistry, T. Melarangi, N.T.N. Vo, D.M. Hoang, C. W. White, C. Denning, S.J. Briddon, S.J. Hill, The use of fluorescence correlation spectroscopy to monitor cell surface β 2-adrenoceptors at low expression levels in human embryonic stem cell-derived cardiomyocytes and fibroblasts, *FASEB J.* 35 (2021), <https://doi.org/10.1096/fj.202002268R>.
- [17] J. Goulding, S.J. Mistry, M. Soave, J. Woolard, S.J. Briddon, C.W. White, B. Kellam, S.J. Hill, Subtype selective fluorescent ligands based on ICI 118,551 to study the human β 2-adrenoceptor in CRISPR/Cas9 genome-edited HEK293T cells at low expression levels, *Pharmacol. Res. Perspect.* 9 (2021), <https://doi.org/10.1002/prp2.779>.
- [18] A. Ishchenko, B. Stauch, G.W. Han, A. Batyuk, A. Shiriaeva, C. Li, N. Zatsepin, U. Weierstall, W. Liu, E. Nango, T. Nakane, R. Tanaka, K. Tono, Y. Joti, S. Iwata, I. Moraes, C. Gati, V. Cherezov, Toward G protein-coupled receptor structure-based drug design using X-ray lasers, *IUCr J* 6 (2019) 1106–1119, <https://doi.org/10.1107/S2052252519013137>.
- [19] M.A.C. Neves, M. Totrov, R. Abagyan, Docking and scoring with ICM: The benchmarking results and strategies for improvement, *J. Comput. Aided Mol. Des.* 26 (2012) 675–686, <https://doi.org/10.1007/s10822-012-9547-0>.
- [20] C. Lanzi, L. Lucarini, M. Durante, S. Sgambellone, A. Pini, S. Catarinichia, D. Łazewska, K. Kiec-Kononowicz, H. Stark, E. Masini, Role of histamine H3 receptor antagonists in intraocular pressure reduction in rabbit models of transient ocular hypertension and glaucoma, *Int. J. Mol. Sci.* 20 (2019) 981, <https://doi.org/10.3390/ijms20040981>.
- [21] M.M. Scharf, M. Zimmermann, F. Wilhelm, R. Stroe, M. Waldhoer, P. Kolb, A Focus on Unusual ECL2 Interactions Yields β 2-Adrenergic Receptor Antagonists with Unprecedented Scaffolds, *Chem. Med. Chem.* 15 (2020) 882–890, <https://doi.org/10.1002/cmdc.201900715>.
- [22] S.R.J. Hoare, P.H. Tewson, A.M. Quinn, T.E. Hughes, A kinetic method for measuring agonist efficacy and ligand bias using high resolution biosensors and a kinetic data analysis framework, *Sci. Rep.* 10 (2020) 1766, <https://doi.org/10.1038/s41598-020-58421-9>.
- [23] C.D. Strader, I.S. Sigal, M. Rios Candelore, E. Rands, W.S. Hill, R.A.F. Dixon, Conserved Aspartic Acid Residues 79 and 113 of the β -Adrenergic Receptor Have Different Roles in Receptor Function, *J. Biol. Chem.* 263 (1988) 10267–10271.
- [24] M. Vass, S. Podlewska, I.J.P. De Esch, A.J. Bojarski, R. Leurs, A.J. Kooistra, C. De Graaf, Aminergic GPCR-Ligand Interactions: A Chemical and Structural Map of Receptor Mutation Data, *J. Med. Chem.* 62 (2019) 3784–3839, <https://doi.org/10.1021/acs.jmedchem.8b00836>.
- [25] P. Loma, A. Guzman-Aranguéz, M.J.P. de Lara, J. Pintor, Beta2 adrenergic receptor silencing change intraocular pressure in New Zealand rabbits, *J Optom* 11 (2018) 69–74, <https://doi.org/10.1016/j.optom.2017.08.002>.
- [26] S. Tsuchiya, T. Higashide, K. Toida, K. Sugiyama, The Role of Beta-Adrenergic Receptors in the Regulation of Circadian Intraocular Pressure Rhythm in Mice, *Curr. Eye Res.* 42 (2017) 1013–1017, <https://doi.org/10.1080/02713683.2016.1264605>.
- [27] P. Kobauri, F.J. Dekker, W. Szymanski, B.L. Feringa, Rational Design in Photopharmacology with Molecular Photoswitches, *Angewandte Chemie - International Edition* 62 (2023), <https://doi.org/10.1002/anie.202300681>.
- [28] J. Broichhagen, J.A. Frank, D. Trauner, A Roadmap to Success in Photopharmacology, *Acc. Chem. Res.* 48 (2015) 1947–1960, <https://doi.org/10.1021/acs.accounts.5b00129>.
- [29] C.P. Page, J. Schaffhausen, N.P. Shankley, The scientific legacy of Sir James W. Black, *Trends Pharmacol Sci* 32 (2011) 181–182, <https://doi.org/10.1016/j.tips.2011.02.009>.
- [30] H.W. Sollinger, Fritz H Bach, Association of high affinity stereospecific binding of 3H-propranolol to cerebral membranes with β adrenoceptors, *Nature* 259 (1976) 488–489. <https://doi.org/10.1038/259488a0>.
- [31] W. Kuipers, R. Link, P.J. Standaar, A.R. Stoit, R. Leurs, A.P. Ijzerman, Study of the Interaction Between Aryloxypropanolamines and Asn386 in Helix VII of the Human 5-Hydroxytryptamine 1A Receptor, 1997. <https://doi.org/10.1124/mol.51.5.889>.
- [32] A.J. Bilski, S.E. Halliday, J.D. Fitzgerald, J.L. Wale, The Pharmacology of a β 2-Selective Adrenoceptor Antagonist (ICI 118,551), *J. Cardiovasc. Pharmacol.* 5 (1983) 430–437, <https://doi.org/10.1097/00005344-198305000-00013>.
- [33] N. Kim, S. Shin, S.W. Bae, cAMP Biosensors Based on Genetically Encoded Fluorescent/Luminescent Proteins, *Biosensors (basel)* 11 (2021) 39, <https://doi.org/10.3390/BIOS11020039>.
- [34] S. Sgambellone, M. Durante, E. Masini, L. Lucarini, Novel Insight of Histamine and Its Receptor Ligands in Glaucoma and Retina Neuroprotection, *Biomolecules* 11 (2020) 1186, <https://doi.org/10.3390/biom11081186>.
- [35] J. Berry, T.K. Lindhorst, G. Despras, Sulfur and Azobenzenes, A Profitable Liaison: Straightforward Synthesis of Photoswitchable Thioglycosides with Tunable Properties, *Chem. A Eur. J.* 28 (2022), <https://doi.org/10.1002/chem.202200354>.
- [36] A. Kerckhoffs, Z. Bo, S.E. Penty, F. Duarte, M.J. Langton, Red-shifted tetra-ortho-halo-azobenzenes for photo-regulated transmembrane anion transport, *Org. Biomol. Chem.* 19 (2021) 9058–9067, <https://doi.org/10.1039/d1ob01457a>.
- [37] M. Wegener, M.J. Hansen, A.J.M. Driessen, W. Szymanski, B.L. Feringa, Photocontrol of Antibacterial Activity: Shifting from UV to Red Light Activation, *J. Am. Chem. Soc.* 139 (2017) 17979–17986, <https://doi.org/10.1021/jacs.7b09281>.
- [38] M. Schehr, C. Ianes, J. Weisner, L. Heintze, M.P. Müller, C. Pichlo, J. Charl, E. Brunstein, J. Ewert, M. Lehr, U. Baumann, D. Rauh, U. Knippschild, C. Peifer, R. Herges, 2-Azo-, 2-diazocine-thiazoles and 2-azo-imidazoles as photoswitchable kinase inhibitors: Limitations and pitfalls of the photoswitchable inhibitor approach, *Photochem. Photobiol. Sci.* 18 (2019) 1398–1407, <https://doi.org/10.1039/c9pp00010k>.
- [39] Y. Xu, C. Gao, J. Andréasson, M. Gröthli, Synthesis and Photophysical Characterization of Azoheteroarenes, *Org. Lett.* 20 (2018) 4875–4879, <https://doi.org/10.1021/acs.orglett.8b02014>.
- [40] E.C.A. Nyns, T. Jin, M.S. Fontes, T. Van Den Heuvel, V. Portero, C. Ramsey, C. I. Bart, K. Zeppenfeld, M.J. Schlij, T.J. Van Brakel, A.A. Ramkisoensing, G. Zhang, R.H. Poelma, B. Ördög, A.A.F. De Vries, D.A. Pijnappels, Optical ventricular cardioversion by local optogenetic targeting and LED implantation in a cardiomyopathic rat model, *Cardiovasc. Res.* 118 (2022) 2293–2303, <https://doi.org/10.1093/cvr/cvab294>.